Molecular Biology of the Cell
Vol. 17, 130–145, January 2006

From Function to Shape: A Novel Role of a Formin in Morphogenesis of the Fungus *Ashbya gossypii*[V]

Hans-Peter Schmitz, Andreas Kaufmann, Michael Köhli, Pierre Philippe Laissue, and Peter Philippsen

Biozentrum der Universität Basel, 4056 Basel, Switzerland

Submitted June 3, 2005; Accepted October 11, 2005
Monitoring Editor: Sandra Schmid

Morphogenesis of filamentous ascomycetes includes continuously elongating hyphae, frequently emerging lateral branches, and, under certain circumstances, symmetrically dividing hyphal tips. We identified the formin *Ag*Bni1p of the model fungus *Ashbya gossypii* as an essential factor in these processes. *Ag*Bni1p is an essential protein apparently lacking functional overlaps with the two additional *A. gossypii* formins that are nonessential. *Agbni1* null mutants fail to develop hyphae and instead expand to potato-shaped giant cells, which lack actin cables and thus tip-directed transport of secretory vesicles. Consistent with the essential role in hyphal development, *Ag*Bni1p locates to tips, but not to septa. The presence of a diaphanous autoregulatory domain (DAD) indicates that the activation of *Ag*Bni1p depends on Rho-type GTPases. Deletion of this domain, which should render *Ag*Bni1p constitutively active, completely changes the branching pattern of young hyphae. New axes of polarity are no longer established subapically (lateral branching) but by symmetric divisions of hyphal tips (tip splitting). In wild-type hyphae, tip splitting is induced much later and only at much higher elongation speed. When GTP-locked Rho-type GTPases were tested, only the young hyphae with mutated *Ag*Cdc42p split at their tips, similar to the DAD deletion mutant. Two-hybrid experiments confirmed that *Ag*Bni1p interacts with GTP-bound *Ag*Cdc42p. These data suggest a pathway for transforming one axis into two new axes of polar growth, in which an increased activation of *Ag*Bni1p by a pulse of activated *Ag*Cdc42p stimulates additional actin cable formation and tip-directed vesicle transport, thus enlarging and ultimately splitting the polarity site.

INTRODUCTION

Elongated cells, such as neurites, pollen tubes, and root hair cells, are generated when polar growth is maintained for extended time periods. An extreme case of polar growth has evolved in filamentous fungi, which are able to extend the tips of their tubelike cells, called hyphae, for unlimited time, provided nutrients are available (Gow, 1995; Momany, 2002; Harris *et al.*, 2005). Hyphae not only very efficiently elongate but regularly establish new axes of polarity along their cortex, thus forming lateral branches, which themselves again generate lateral branches. This results in a fast spreading network of hyphae and the typical appearance of a fungal mycelium. In most filamentous fungi the initial hyphal tip elongation speed can increase by an order of magnitude or even more. Some filamentous fungi display hyphal tip splitting, the unique ability to simultaneously generate at tips of fast growing hyphae two sister hyphae.

The ascomycete *Ashbya gossypii* shows all the hallmarks of fungal filamentous growth, including tip splitting, although its recently completed genome sequence reveals an evolutionary relation with the *Saccharomyces cerevisiae* genome (Dietrich *et al.*, 2004). *A. gossypii* is amenable to functional genome analysis using gene targeting methods or autonomously replicating plasmids (Wright and Philippsen, 1991; Steiner and Philippsen, 1994; Steiner *et al.*, 1995; Wendland *et al.*, 2000), which have promoted functional analyses of polarity genes in this fungus. Polar growth in *A. gossypii* starts from an isotropically growing germ bubble. The first steps in polarity establishment involve the *A. gossypii* proteins *Ag*Cdc24p and *Ag*Cdc42p (Wendland and Philippsen, 2001). Once the first germ tube has emerged hyphal growth of *A. gossypii* proceeds with frequent lateral branching and a steadily increasing elongation speed from initially 5 μm/h up to a maximum of 170 μm/h (Knechtle *et al.*, 2003). For this process of hyphal maturation *Ag*Bem2p, *Ag*Rho3p, *Ag*Cla4p, *Ag*Spa2p, and *Ag*Rsr1p are important (Ayad-Durieux *et al.*, 2000; Wendland and Philippsen, 2000, 2001; Knechtle *et al.*, 2003; Bauer *et al.*, 2004). Although *Ag*Bem2p, *Ag*Rho3p and *Ag*Rsr1p are responsible for maintenance of polarity, both *Ag*Cla4p and *Ag*Spa2p are necessary to reach maximal growth speed.

An important late step in the development to a fast spreading *A. gossypii* mycelium is the splitting of hyphal tips which, under optimal growth conditions, begins 12–14 h after emergence of the first hypha (Ayad-Durieux *et al.*, 2000). A study with a GFP-labeled *Ag*Spa2p showed that during tip splitting the existing polarity control center divides into two new centers of polarity, yielding two hyphae that elongate, after a short lag phase, with a speed similar to that before tip splitting (Knechtle *et al.*, 2003). So far, the molecular basis for the initiation of hyphal tip splitting is unknown. We assumed that the apparent duplication of polar growth capacity depends on an approximately twofold increase in secretory vesicle transport at or shortly after

This article was published online ahead of print in *MBC in Press* (http://www.molbiolcell.org/cgi/doi/10.1091/mbc.E05–06–0479) on October 19, 2005.

[V] The online version of this article contains supplemental material at *MBC Online* (http://www.molbiolcell.org).

Address correspondence to: Peter Philippsen (peter.philippsen@unibas.ch).

tip splitting and that, before this increase, additional tip-located actin cables had to form. Given the conserved role of formins in nucleating actin cables (Pruyne *et al.*, 2002; Sagot *et al.*, 2002b), we therefore hypothesized that a formin homolog could play an important role for the regulation of tip splitting.

Formins are common to all eukaryotic species and participate in many different processes, from cell polarization to embryonic development (see Wallar and Alberts (2003) and Evangelista *et al.* (2003) for reviews). Except for some cases in higher cells where a formin is involved in signaling (Habas *et al.*, 2001), most formins participate in the organization of the actin cytoskeleton. Recently, the ability of formins to nucleate actin at the barbed end of actin filaments was described for different organisms (Pruyne *et al.*, 2002; Sagot *et al.*, 2002b; Kobielak *et al.*, 2003; Kovar *et al.*, 2003; Li and Higgs, 2003). Actin nucleation is mediated by the conserved formin homology domain FH2. As found by analyzing the crystal structures of the mouse formin, mDIA, and the yeast formin, *Sc*Bni1p, the core of the FH2 domain seems to have actin binding capacity, whereas adjacent amino acids are necessary for oligomerization and gain of polymerization capability (Shimada *et al.*, 2004; Xu *et al.*, 2004). A subclass of formins, the so-called diaphanous related formins (DRFs), are defined by two properties: First, they are activated when a GTP-bound Rho-type protein interacts with their amino terminus (Kohno *et al.*, 1996; Evangelista *et al.*, 1997; Imamura *et al.*, 1997; Watanabe *et al.*, 1997; Habas *et al.*, 2001). Second, they posses a carboxy-terminal diaphanous autoregulatory domain (DAD), which binds to the amino-terminus in the inactive state of these formins (Watanabe *et al.*, 1999; Alberts 2001).

In fungi, six formins have been studied to date. In *S. cerevisiae*, the two formins Bni1p and Bnr1p are required for cell polarity and cytokinesis with some overlapping and some different functions (Zahner *et al.*, 1996; Evangelista *et al.*, 1997; Imamura *et al.*, 1997; Kamei *et al.*, 1998; Pruyne *et al.*, 2004). In *Schizosaccharomyces pombe*, three formins exist which are also involved in cell polarity and cytokinesis. The protein *Sp*Cdc12p is involved in cytokinesis (Chang *et al.*, 1997; Kovar *et al.*, 2003), *Sp*Fus1p in cell fusion (Petersen *et al.*, 1998b) and *Sp*For3p in cell polarity control via regulation of the actin and microtubule network (Feierbach and Chang, 2001; Nakano *et al.*, 2002). The only formin family member described so far in a filamentous fungus is the SepA protein of *Aspergillus nidulans*. SepA is an essential protein that locates to growing hyphal tips and to sites of cytokinesis (septation). Some SepA mutants still grow in a filamentous manner although they can no longer form septa (Harris *et al.*, 1997; Sharpless and Harris, 2002).

In this article we first document by videomicroscopy the distinct differences in polar growth of budding yeast and *A. gossypii* and compare the domain compositions of the three *A. gossypii* formins with the two *S. cerevisiae* formins. Then we show that mutants lacking the *Ag*Bnr1p or *Ag*Bnr2p formin develop like wild type and that mutants lacking both formins are unable to grow. We next provide evidence that the *Ag*Bni1p formin is essential for hyphal emergence and elongation, that it localizes at hyphal tips, and that it is essential for organization of actin cables and thus tip-directed transport of secretory vesicles. In addition, we demonstrate that constitutively active *Ag*Bni1p leads to premature tip splitting and that this is most likely triggered by *Ag*Cdc42p-GTP.

MATERIALS AND METHODS

A. gossypii Strains and Growth Conditions

All strains were constructed by PCR-based gene targeting according to the method described by Wendland *et al.* (2000). Either pGEN3 (Wendland *et al.*, 2000), pGUG (Knechtle *et al.*, 2003), or pUC19NATPS (D. Hoepfner, personal communication) were used as templates to generate gene-targeting cassettes encoding geneticin-resistance, GFP plus geneticin-resistance, and ClonNAT-resistance, respectively. Strains and names of the oligonucleotides and templates used are given in Table 1. The strains were verified by PCR using a PTC 100 thermocycler (MJ Research, Waltham, MA). All oligonucleotides are listed in Table 2. Strains were grown at 30°C in AFM (Ashbya Full Medium) with or without geneticin or ClonNAT or at room temperature on synthetic medium for live cell imaging (Knechtle *et al.*, 2003).

DNA Manipulations and Sequencing

All DNA manipulations were carried out according to Sambrook *et al.* (2001) with DH5αF′ as host (Hanahan, 1983). Sequencing was done using an ABI prism 377 DNA sequencer (PE Applied Biosystems, Foster City, CA) according to the manufacturer's instructions. Plasmids were isolated from yeast using the High Pure Plasmid Purification Kit (Roche Diagnostics, Mannheim, Germany) according to the instruction manual for plasmid preparation from *Escherichia coli* but with the following modifications: 5 ml of a yeast culture was collected by centrifugation and the supernatant was discarded. The cells were resuspended in solution 1 and 0.2 g of 0.5-mm glass beads were added. Cells were lysed by vortexing for 8 min at 4°C. From here on the instructions of the manufacturer were followed, only the elution volume was decreased to 20 μl. Ten microliters of the elute were transformed into *E. coli* for plasmid amplification.

Plasmids and Constructs

All plasmids are listed in Table 3. All constructs carrying genes for Rho-type GTPases were constructed using the same scheme. Each gene was amplified from *A. gossypii* genomic DNA using the corresponding primers from Table 2 for PCR. All primers were designed to amplify the open reading frame (ORF) from the start codon to the end, excluding the nucleotides coding for the CAAX motif at the carboxy terminus, thus avoiding lipid modification (primers AgRHOx-ATG, AgRHOx-TAG and AgCDC42-ATG, and AgCDC42-TAG). To facilitate cloning, *Eco*RI and *Bam*HI restriction sites were added to the oligonucleotides. The fragments were purified, cut, and ligated into pUC19 (Vieira and Messing, 1991). Activated alleles of all Rho-GTPases were constructed using the method by Boles and Miosga (1995) with primers named AgRHOx and AgCDC42 plus the corresponding nucleotide exchange. DNA of wild-type and mutant alleles was cloned into pGBT9 (Bartel *et al.*, 1993) using again *Eco*RI and *Bam*HI. The resulting plasmids were verified by sequencing. *AgBNI1* was amplified by PCR from genomic *A. gossypii* DNA using primers AgBNI1-ATG2Hy and AgBNI1-TAG2Hy, which add on both sides of the amplified *AgBNI1* 45 base pairs homologous to pGBT9 for in vivo cloning. This PCR product was cotransformed with *Eco*RI- and *Bam*HI-digested pGBT9 into the yeast strain DHD5. Transformants were restreaked on selective medium, and recombinant plasmids were isolated from the yeast cells and amplified in *E. coli*. This resulted in pGBT9AgBNI1. From this, a 2.5-kb *Eco*RI-*Bgl*II fragment was cut out and ligated into the *Eco*RI-*Bam*HI sites of pGAD424 (Bartel *et al.*, 1993). Again the plasmid was first verified by digestion and sequencing.

The plasmid carrying *AgBNI1* (pAMK1) was constructed by ligation of an *Hin*dIII/*Sma*I fragment generated by PCR using primers AgBNI1-P_HindIII and AgBNI1-T_SmaI from genomic *A. gossypii* DNA. *GFP* was fused to the gene by in vivo recombination in *S. cerevisiae* strain DHD5 with a PCR fragment derived from pGUG with primers AgBNI1-GS1 and AgBNI1-GS2. The fusion was verified by sequencing.

An amino-terminal fusion of *Ag*SEC4 to GFP was constructed by a sequential series of PCR amplification and cloning steps. First, the *AgSEC4* promoter was amplified by PCR out of the genome using primers Sec4P-Hind and Sec4P-Bam and cloned into YCPlac111 using *Hin*dIII and *Bam*HI. The resulting plasmid was cut with *Bam*HI and *Eco*RI to allow fusion of the *SEC4* promoter to GFP that was amplified by PCR from pGUG with primers GFP-Eco and GFP-Bam. In a final step the *AgSEC4* ORF and terminator were fused to the GFP-ORF using the enzymes *Eco*RI and *Spe*I and a fragment generated from genomic DNA using primers Sec4-Eco and Sec4-Spe.

The $S_{1642}G$ allele of *AgBNI1* was generated using the method described by Storici *et al.* (2001) using primers Agbni1–12C1, Agbni1–12C2, Agbni1–12IRO1, and Agbni1–12IRO2 and *S. cerevisiae* strain CEN/PK2 (http://www.rz.uni-frankfurt.de/FB/fb16/mikro/euroscarf/) transformed with pAMK1. The resulting plasmid pAMK1ts12 was isolated from yeast digested with *Asc*I and dephosphorylated. The linearized vector was cotransformed together with a PCR product generated with primers AgBNRCFP-N and AgBNI1-GS2 from pGUG for in vivo recombination to integrate the *URA3* terminator from *S. cerevisiae* behind the mutagenized *Agbni1* gene. The resulting vector was isolated and verified by sequencing of the altered regions. An *Xba*I fragment containing the altered region of *AgBNI1*, the *URA3* terminator and the G418 resistance cassette was cloned into pUC19. The resulting plas-

Table 1. *Ashbya gossypii* strains and details of construction

Strain	Genotype	Oligo-nucleotides	Template	Reference
ATCC10895	Wild type	—	—	Ashby and Nowell (1926)
Δl Δt	*Agleu2Δ Agthr4Δ*	—	—	Altmann-Johl and Philippsen (1996)
Agbni1Δ2	*Agbni1Δ::GEN3, Agleu2Δ Agthr4Δ*	AgBNI1-S1 AgBNI1-S2	pGEN3	This study
AgBNI1ΔD	*AgBNI1Δ5308–5757::GEN3*	AgBNI1dD-S1 AgBNI1dD-S2	pGEN3	This study
AgBNI1-GFP	*AgBNI1-GFP-GEN3, Agleu2Δ Agthr4Δ*	AgBNI1-GS1 AgBNI1-GS2	pGUG	This study
AgSPA2-GFP	*AgSPA2-GFP-GEN3, Agleu2Δ Agthr4Δ*	—	—	Knechtle *et al.* (2003)
Agbni1Δ AgSPA2-GFP	*Agbni1Δ::NAT1, AgSPA2-GFP-GEN3, Agleu2Δ Agthr4Δ*	AgBNI1-NS1 AgBNI1-NS2	pUC19NATPS	This study
Agbni1S$_{1642}$G	*Agbni1T4924G, C4925G-GEN3, Agleu2Δ Agthr4Δ*	See text for details		This study
Agbni1Δ$_{1530}$G, K$_{1620R}$	*Agbni1A4589G, A4859G-GEN3, Agleu2Δ Agthr4Δ*	See text for details		This study
Agbnr1Δ-GEN3	*Agbnr1Δ::GEN3, Agleu2Δ Agthr4Δ*	AgBNR1-S1 AgBNR1-S2	pGEN3	This study
Agbnr1Δ-NAT1	*Agbnr1Δ::NAT1, Agleu2Δ Agthr4Δ*	AgBNR1-NS1 AgBNR1-NS2	pUC19NATPS	This study
Agbnr2Δ	*Agbnr2Δ::GEN3, Agleu2Δ Agthr4Δ*	AgBNR2-S1 AgBNR2-S2	pGEN3	This study
Agbnr1,2ΔGL	*Agbnr1Δ::GEN3, Agbnr2Δ::LEU2, Agleu2Δ Agthr4Δ*	AgBNR2-S1 AgBNR2-S2	pScLEU2	This study
Agbnr1,2ΔGN	*Agbnr1Δ::GEN3, Agbnr2Δ::NAT1*	AgBNR1-NS1 AgBNR1-NS2	pUC19NATPS	This study
*Agcdc42**	*Agcdc42G183C-GEN3, Agleu2Δ Agthr4Δ*	See text for details		This study
AgBNI1ΔD-GFP	*AgBNI1ΔD-GFP-GEN3, Agleu2Δ Agthr4Δ*	AgBNI1dD-F1 AgBNI1dD-F2	pAGT141	This study

mid pHPS232 was cut again with *Xba*I and transformed into the *A. gossypii* Δ*l*Δ*t* strain. Construction of the D$_{1530}$R,K$_{1620}$R allele of *AgBNI1* was identical to the S$_{1642}$G allele except for a sequential round of mutagenesis first using primers Agbni1–11.1C1, Agbni1–11.1C2, Agbni1–11.1IRO1 and Agbni1–11.1IRO2 and Agbni1–11.2C1, Agbni1–11.2C2, Agbni1–11.2IRO1 and Agbni1–11.2IRO2 respectively.

For construction of the Q$_{61}$H allele of *AgCDC42* the gene was first PCR-amplified from genomic *A. gossypii* DNA using primers cdc42genom_sense and cdc42genom_antisense. The resulting product was cut with *Eco*RV, and *Pst*I was ligated into pRS415 cut with *Sma*I and *Pst*I. In the resulting plasmid pCDC42 the codon CAG starting at position 181 was deleted by integration of the pCORE-cassette (Storici *et al.*, 2001) using primers AgCdc42_Q-H-sense and AgCdc42_Q-H-antisense. This resulted in plasmid pCDC42cas. By homologous recombination in yeast with annealed primers and counterselection, the pCORE-cassette was replaced by the mutagenized codon, resulting in pcdc42cons. The Gen3 resistance cassette was amplified from pGEN3 using primers INT_CDC42*_S1 and INT_CDC42*_S2. The resulting PCR product was integrated behind the *cdc42* gene in the vector pcdc42cons yielding pcdc42kanr. The 3.1-kb *Bam*HI/*Pst*I fragment from pcdc42kanr carrying the mutagenized *cdc42* and the resistance cassette was cloned into pUC19, resulting in pUC19cdc42cons. DNA of this vector was again cut with *Bam*HI/*Pst*I and transformed into *A. gossypii*. Transformants resistant against G418 were sporulated and spores were separated to get homokaryotic Geneticin (G418) resistant mycelium. From this mycelium the *CDC42* gene was amplified by PCR using primers AgCDC42-ATG and AgCDC42-TAG. The resulting PCR product was sequenced to verify the presence of the desired mutation.

Image Acquisition and Processing

The microscopy setup used was the same as described in Knechtle *et al.* (2003). Actin staining was done according to Knechtle *et al.* (2003). The illumination time and light intensity for standard phase contrast, DIC, or fluorescence acquisitions was chosen to reach minimally 25% of the maximal intensity. For multiple exposures of the same sample bleaching of the sample had to be taken into account. The *Z*-distance between two planes in stack acquisitions was set between 0.1 and 0.5 μm. Phase contrast, DIC, and single-plane fluorescence images were processed using the "scale image" and "unsharp mask" feature in MetaMorph (Universal Imaging, West Chester, PA). Stacks were deblurred with MetaMorph's "remove haze," flattened by maximum projection with "stack arithmetics" and scaled as mentioned above. Fluorescence and phase-contrast images were colored and overlaid using MetaMorph's "overlay images" tool. For time-lapse acquisition spores were cultured on a slide with a cavity (time-lapse slide) that was filled with solid medium (Ashbya Full Medium). Spores were incubated in a humid chamber without coverslip until they reached the required developmental stage. Then a coverslip was applied. For Supplementary Movies S1 to S7 cells or spores were cultured on Petri plates with AFM agar, cultivated in a humid chamber, and placed for image acquisitions under a light microscope. The acquisition frequency varied between 1 and 0.2 min^{-1}. The time-lapse picture series were exported from MetaMorph as 8-bit TIFF files converted to a QuickTime (Apple Computer, Redmond, WA) or AVI movie with Adobe Premiere 4.2 (Adobe Systems, San Jose, CA).

Two-hybrid Experiments

For two-hybrid experiments prey and bait plasmids were cotransformed into *S. cerevisiae* strain PJ69-4a (James *et al.*, 1996) and selected on minimal medium lacking leucine and tryptophan but containing a fourfold concentration (80 mg/l) of adenine. Transformants were grown in the same liquid medium to an OD$_{600}$ of ~1. Of these, 5 μl were spotted on plates lacking in addition to leucine and tryptophan either histidine or adenine to monitor activity of the reporter genes.

RESULTS

Filamentous Growth of A. gossypii Compared with Unicellular Growth of S. cerevisiae

A. gossypii grows like a filamentous ascomycete (Momany, 2002) and the main differences to yeastlike growth are shown in Figure 1A. Sustained polar growth results in continuous tip extensions of hyphae and lateral branches. Thus, growth of the hyphal surface is restricted to the tips, and isotropic growth phases are absent. In a yeast cell, a short phase of polar growth of the emerging bud is followed by isotropic growth of the bud. Then a septum grows at the junction between the mother cell and the bud and both cells

Table 2. Oligonucleotides used in this study

Name	Sequence[a]	Purpose
AgBNI1-S1	CTCGACCGTAGAGTCGATAGCGAGTTCTGCTCTAGCAAAATCCCCGCTAGGGATAACAGGGTAAT	Deletion
AgBNI1-S2	GAGTTGTTCGATGGAGATCTTGACCACCTGAAGTACAGGTTCAAGAGGCATGCAAGCTTAGATCT	Deletion
AgBNI1-G1	CCCGACCACCGTCTTGGACC	Verification
AgBNI1-G2	GGGCATTTGCGCCGGGAGAG	Verification
AgBNI1-GS1	CGGTGAACACCCGGAGTCTCGCAAGTCAATGCTCGATGAGCACAAGGGTGCAGGCGCTGGAGCTG	GFP-tagging
AgBNI1-GS2	GCGGCGCGGCGGCGACATCGCGCTGGTCTATCAGTTTCTTGGTGCGGCAGGGACCTGGCACGGAGC	GFP-tagging
AgBNI1-I1	CAGATCGGGCCTGTGTTACC	Verification
AgBNR2-S1	GATAAAGAACATCGCTAGTTAATTTTGCTAATAAAGAAGAGACCTTTAAgctagggataacagggtaat	Deletion
AgBNR2-S2	GGCCGATAAGTGTGGAATCGGATAAGTGTTGAATAGGGTAACGGAAGAGGCATGCAAGCTTAGATCT	Deletion
AgBNR2-I1	CGCACTCCGCACCGTGGACC	Verification
BNR2G1neu	CTGTCGAGGAATTAACTTTAAG	Verification
BNR2G2neu	GCCAGCGCATTTTGCACCGG	Verification
AgBNR1-S2	GCCCGAGCGCCGAAGGCGAAGGGATGCGAAAAGTATATAGATGCAAGTTGaggcatgcaagcttagatct	Deletion
AgBNR1-S1	GCGGGAGCAGTAGATTTGTGCCTGGGCCCCTCCCCCGCGAGTGCGCAATGgctagggataacagggtaat	Deletion
AgBNR1-I1	CAGGCTGTGCGGCGCGCGCG	Verification
BNR1G1neu	GAGCAGCTGGTCGCTGGGCATCTCGTGG	Verification
BNR1G4neu	GCCTCGAATCACCAATCCCC	Verification
AgBNR1-NS1	GGCGGGAGCAGTAGATTTGTGCCTGGGCCCCTCCCCCGCGAGTGCGCAccagtgaattcgagctcgg	Deletion
AgBNR1-NS2	GCCCGAGCGCCGAAGGCGAAGGGATGCGAAAAGTATATAGATGCAAGTTG tacgccaagcttgcatgcct	Deletion
V2PDC1P	GAACAAACCCAAATCTGATTGCAAGGAGAGTGAAAGAGCCTT	Verification
V3PDC1T	GACCAGACAAGAAGTTGCCGACAGTCTGTTGAATTGGCCTG	Verification
AgBNI1dD-S1	TCTGGAGTACAAGCGCGCGCAGGAGTTTAACCGCAAGATCTAAGCTAGGGATAACAGGGTAAT	Deletion
AgBNI1dD-S2	GCTGGTCTATCAGTTTCTTGGTGCGGCGCTGGCGAACCTTAGGCATGCAAGCTTAGATCT	Deletion
Agbni1-12 C1	CTTGAACTACGTGGAACGCATCGTCAGCCAGAATTATCCAgagctcgttttcgacactgg	pCORE integration
Agbni1-12 C2	CCTGAAGTACAGGTTCAAGTTCCTGGAGAAAGCTGTTGAAtccttaccattaagttgatc	pCORE integration
Agbni1-12 IRO1	ATGACTTTCTTGAACTACGTGGAACGCATCGTCAGCCAGAATTATCCAGGGTTCAACAGC	Mutagenesis
Agbni1-12 IRO2	TTGACCACCTGAAGTACAGGTTCAAGTTCCTGGAGAAAGCTGTTGAACCCTGGATAATTC	Mutagenesis
Agbni1-11.1 C1	TAAGTCTCCGGAAAAGGATCCAAGCGAGCTTCAGCGATCAgagctcgttttcgacactgg	pCORE integration
Agbni1-11.1 C2	AGTAGCTTTGAAGATTAACAATGAGGTTCAAGAATAACTGtccttaccattaagttgatc	pCORE integration
Agbni1-11.1 IRO1	GAGGATGCTAAGTCTCCGGAAAAGGATCCAAGCGAGCTTCAGCGATCAGGCCAGTTATTC	Mutagenesis
Agbni1-11.1 IRO2	TGAGCTCCAGTAGCTTTGAAGATTAACAATGAGGTTCAAGAATAACTGGCCTGATCGCTG	Mutagenesis
Agbni1-11.2 C1	GGGGTTCAAGTTGAGTACATTGCAGAGGCTCACCTTCATTgagctcgttttcgacactgg	pCORE integration
Agbni1-11.2 C2	GTTCCACGTAGTTCAAGAAAGTCATGCTGTTTTTCTCGTCtccttaccattaagttgatc	pCORE integration
Agbni1-11.2 IRO1	GCACAGGGGTTCAAGTTGAGTACATTGCAGAGGCTCACCTTCATTAGAGACGAGAAAAAC	Mutagenesis
Agbni1-11.2 IRO2	CTGACGATGCGTTCCACGTAGTTCAAGAAAGTCATGCTGTTTTTCTCGTCTCTAATGAAG	Mutagenesis
AgBNRCFP-N	CCAGCATGTCAACCACTATATTGATCACCGATATATGGACTTCCACACCAACTAGacgcggccgccagctgaagc	In vivo recombination
AgBNI1-GS2	GCGGCGCGGCGGCGACATCGCGCTGGTCTATCAGTTTCTTGGTGCGGCagggacctggcacggagc	In vivo recombination
AgRHO1a-ATG	GAGATCGAATTCATGGCGTACCAGACAGGCGGCA	Cloning
AgRHO1aG204C	GCCGGTCGTAGTCCTCcTGGCCCGCTGTATCCC	Mutagenesis
AgRHO1a-TAG	CGACGGATCCCTTTCTTCTTCTTCTTGTCACCGT	Cloning
AgRHO1b-ATG	GATCGAATTCATGTCTCAGCAAATGCATAAC	Cloning
AgRHO1bG207C	GCCTGTCGTAATCCTCGTGCCCAGCCGTATCC	Mutagenesis
AgRHO1b-TAG	CGACGGATCCCCTTTTTCTTCTTCTTCTTGTCAGAC	Cloning
AgRHO2-ATG	GAGATCGAATTCATGACGGTCAACGTTGTGAGAC	Cloning
AgRHO2G195C	CAGACGCTCGTATTCTTCGTGACCAGCAGTATCC	Mutagenesis
AgRHO2-TAG	CGACGGATCCCGCCTTGACCCGGCTCCTTGTTCAC	Cloning
AgRHO3-ATG	GATCGAATTCATGCCTCTGTGTGGGTCGAG	Cloning
AgRHO3G219C	GCAACCGGTCAAACTCCTCGTGCCCAGCAGTGTCCCACAGG	Mutagenesis
AgRHO3-TAG	GACGGATCCCACTGCTGCTTTCGGCCTCGG	Cloning
AgRHO4-ATG	GAGATCGAATTCATGAGCGCAGGGCCGTTGCAAG	Cloning
AgRHO4G333C	CAGCCGGCTGTACTCCTCGTGCCCAGCAGTGTCCCACAGC	Mutagenesis
AgRHO4-TAG	GACGGATCCCGCGGTGCTTGCGCACCCGCTTG	Cloning
AgRHO5-ATG	GATCGAATTCATGTGTTTTTCGCAGAGCGGCAG	Cloning
AgRHO5G255Cneu	CCGCAACCGGTCGTACTCCTCGTGCCCCGCCGTGTCCCACAG	Mutagenesis
AgRHO5-TAG	CGACGGATCCCTCTAGATCTCTTCCTCCTCTTTTTC	Cloning
AgCDC42-ATG	GATCGAATTCATGCAGACATTGAAGTGCGTGGTC	Cloning
AgCDC42-TAG	CGACGGATCCCCTTCTTGCTCTTCTTGATG	Cloning
AgCDC42G183C	GCCGCAACCTGTCGTAGTCCTCGTGGCCGGCAGTGTCGAACAAGC	Mutagenesis
u-40	GTTTTCCCAGTCACGAC	Mutagenesis
Reverse	CAGGAAACAGCTATGACCATG	Mutagenesis
Sec4-ECO	cgcgaattcTCGGGGCTAAGAACGGTGTC	Cloning
Sec4P-BAM	ccggatccCATTATAGCTACTGTACTGC	Cloning
Sec4P-HIND	ggaagcttCTACTACGCCTGAGCGCCGC	Cloning
Sec4-SPE	caccaactagtTGGGCGGCCTGTGCTGCAAAG	Cloning
GFP-BAM	cgggatccAGTAAAGGAGAAGAACTTTTCAC	Cloning
GFP-ECO	cgcgaattcTTTGTATAGTTCATCCATGCC	Cloning
AgBNI1-ATG2Hy	GTAGTAACAAAGGTCAAAGACAGTTGACTGTATCGCCGGAATTCatgaagaagtccacgcactcgaac	In vivo recombination
AgBNI1-TAG2Hy	CATAAGAAATTCGCCCGGAATTAGCTTGGCTGCAGGTCGACGGATCCttacttgtgctcatcgagcattg	In vivo recombination
AgBNI1-P_HindIII	gcgcgcaagcttCTGGGACGACGACAAGCCTAC	Cloning
AgBNI1-T_SmaI	gcgccccgggCCTGCACCGAAATCCGCCGA	Cloning
AgBNI1-GS1	CGGTGAACACCCGGAGTCTCGCAAGTCAATGCTCGATGAGCACAAGggtgcaggcgctggagctg	In vivo recombination
AgBNI1-GS2	GCGGCGCGGCGGCGACATCGCGCTGGTCTATCAGTTTCTTGGTGCGGCagggacctggcacggagc	In vivo recombination
AgBNI1-NS1	GGTATAGTGGCAGCGTCGGCGGCTGGGCACATATGCAAGGccagtgaattcgagctcgg	Deletion
AgBNI1-NS2	GCTGGTCTATCAGTTTCTTGGTGCGGCGCTGGCGAACCTTtacgccaagcttgcatgcct	Deletion
Gal4-ad	GTTTGGAATCACTACAGGG	sequencing
Gal4-bd	GATTGGCTTCAGTGGAG	sequencing
Gad-term	GAGATGGTGCACGATGCACAGTTG	sequencing
Gbt-term	CGTTTTAAAACCTAAGAGTCAC	sequencing
AgCdc42_c1	GGACGAGCCGTACACGTTGGGCTTGTTCGACACTGCCGGGgagctcgttttcgacactgg	pCORE integration
AgCdc42_c2	GTCGACGGGTACGACAACGGCCGCAACCTGTCGTAGTCCTCtccttaccattaagttgatc	pCORE integration
AgCdc42_Q-H-antisense	cacgtccgtcgacgggtacgacaacggccgcaacctgtcgtagtcctcgtgcccggcagtg	Mutagenesis
AgCdc42_Q-H-sense	gtgatgatcggggacgagccgtacacgttgggcttgttcgacactgccgggcacgaggac	Mutagenesis
INT_CDC42*_S1	ACCAAGTGCCAGCTCTAGCGCCAGGACCCGCGCGAGACCTGCTAGGGATAACAGGGTAAT	Mutagenesis
INT_CDC42*_S2	TTGCCGATTTTTGGGCAGGGCGCAAAGACAGATATAGCAGAGGCATGCAAGCTTAGATCT	Mutagenesis
AgCDC42-ATG	GATCGAATTCATGCAGACATTGAAGTGCGTGGTC	Verification
AgCDC42-TAG	CGACGGATCCCCTTCTTGCTCTTCTTGATG	Verification
AgBNI1dD-F1	GACTTTATTCTGGAGTACAAGCGCGCGCAGGAGTTTAACCGCAAGATCaaaacgacggccagtgaattcg	In vivo recombination
AgBNI1dD-F2	GACATCGCGCTGGTCTATCAGTTTCTTGGTGCGGCGCTGGCGAACCTTaccatgattacgccaagcttgc	In vivo recombination

[a] Underscore indicates nucleotides exchanged for mutagenesis.

Table 3. Plasmids

Name	Insert	Reference
pUC19	—	Vieira and Messing (1991)
pGBT9	—	Bartel *et al.* (1993)
pGAD424	—	Bartel *et al.* (1993)
YCPlac111	—	Gietz and Sugino (1988)
pRS415	—	Sikorski and Hieter (1989)
pUC19NATPS	—	D. Hoepfner, personal communication
pAGT141	pUC19 carrying the *Pst*I fragment from pGEN and the *Sac*I fragment from pGUG	A. Kaufmann, personal communication
pCORE	—	Storici *et al.* (2001)
pUC19AgRHO1a	*A. gossypii RHO1a* from nucleotide 1–615	This study
pUC19AgRHO1b	*A. gossypii RHO1b* from nucleotide 1–609	This study
pUC19AgRHO2	*A. gossypii RHO2* from nucleotide 1–546	This study
pUC19AgRHO3	*A. gossypii RHO3* from nucleotide 1–660	This study
pUC19AgRHO4	*A. gossypii RHO4* from nucleotide 1–765	This study
pUC19AgRHO5	*A. gossypii RHO5* from nucleotide 1–870	This study
pUC19AgCDC42	*A. gossypii CDC42* from nucleotide 1–561	This study
pGBTAgRHO1a	*A. gossypii RHO1a* from nucleotide 1–615	This study
pGBTAgRHO1b	*A. gossypii RHO1b* from nucleotide 1–609	This study
pGBTAgRHO2	*A. gossypii RHO2* from nucleotide 1–546	This study
pGBTAgRHO3	*A. gossypii RHO3* from nucleotide 1–660	This study
pGBTAgRHO4	*A. gossypii RHO4* from nucleotide 1–765	This study
pGBTAgRHO5	*A. gossypii RHO5* from nucleotide 1–870	This study
pGBTAgCDC42	*A. gossypii CDC42* from nucleotide 1–561	This study
pGBTAgRHO1a*	*A. gossypii RHO1a* G204C from nucleotide 1–615	This study
pGBTAgRHO1b*	*A. gossypii RHO1b* G207C from nucleotide 1–609	This study
pGBTAgRHO2*	*A. gossypii RHO2* G195C from nucleotide 1–546	This study
pGBTAgRHO3*	*A. gossypii RHO3* G219C from nucleotide 1–660	This study
pGBTAgRHO4*	*A. gossypii RHO4* G333C from nucleotide 1–765	This study
pGBTAgRHO5*	*A. gossypii RHO5* G255C from nucleotide 1–870	This study
pGBTAgCDC42*	*A. gossypii CDC42* from nucleotide 1–561	This study
pGBTAgBNI1-N	*A. gossypii BNI1* from nucleotide 1–3152	This study
pGADAgBNI1-N	*A. gossypii BNI1* from nucleotide 1–3152	This study
YCp111GFPSEC4	N-terminal Fusion of *GFP* to *A. gossypii SEC4*	This study
pAMK1	*A. gossypii BNI1* from nucleotide −682 to +523	This study
pCDC42	*AgCDC42* including promoter and terminator	This study
pCDC42cas	*Agcdc42* with codon CAG starting at position 181 replaced by pCORE	This study
pcdc42cons	pCDC42 with codon CAG starting at position 181 altered to CAC	This study
pcdc42kanr	pcdc42cons with integrated GEN3 cassette behind ORF	This study
pUC19cdc42cons	3.1 kb *Bam*HI/*Pst*I fragment from pcdc42kanr with pUC19 backbone	This study
pSEC4NAT	*Pst*I fragment from pUC19NATPS carrying ClonNAT cassette ligated into *Pst*I site of YCP111GFPSEC4. Orientation reverse	This study

separate. Septation in *A. gossypii* like in other filamentous ascomycetes occurs in the growing hyphae and at the base of branches but separation of hyphal segments does not occur. Lateral branching leads to the successive establishment of several novel axes of polarity at the cortex of growing hyphae, in *A. gossypii* usually in an about right angle from the growth axis of the mother hyphae. In budding yeast, only one novel axis of polarity (site of bud emergence) is established in each cell cycle. Finally, the process of dividing the polarity-axis at the tip of mature hyphae (tip splitting) is restricted to a subset of filamentous ascomycetes including *A. gossypii*. Budding yeasts do not simultaneously generate two buds (two axes of polarity).

To visualize the differences in growth dynamics of *S. cerevisiae* and *A. gossypii*, we simultaneously monitored, by time-lapse video microscopy, growth of both fungi on AFM agar (Movie S1). Four representative frames were selected to show the development of *S. cerevisiae* mini colonies and of an *A. gossypii* mycelium (Figure 1B). Arrows in the zero minute frame point to eight *S. cerevisiae* cells, which have just finished the first division, and to one germinated *A. gossypii* spore from which the first hypha has emerged. After 225 min, the *S. cerevisiae* cells have undergone only one or two additional divisions whereas the *A. gossypii* young mycelium has already developed nine growing hyphae. At 450 min, the *S. cerevisiae* cells have divided one or two more times, and the *A. gossypii* young mycelium is now spreading from 23 hyphal tips. After nearly 700 min, the fastest hyphae (marked with open arrow heads) have started to symmetrically divide at their tips, the common mode of branching when hyphal tip speeds have reached 80 μm/h or more. This switch in branching pattern allows optimal radial spreading of an *A. gossypii* mycelium. The apparently symmetric division of the polar growth machinery leads only to a transient decrease of tip elongation speeds by ~20% as determined for seven tip splitting events in Supplementary Movie S1 (unpublished data). Using similar conditions, Knechtle *et al.* (2003) presented the dynamics of successive tip splitting events every 90–120 min at the edge of a radially expanding mature *A. gossypii* mycelium.

How can these differences in morphogenesis be explained when both organisms carry a very similar set of proteins? One possible answer is that homologous polar growth components may exert not only common functions but also

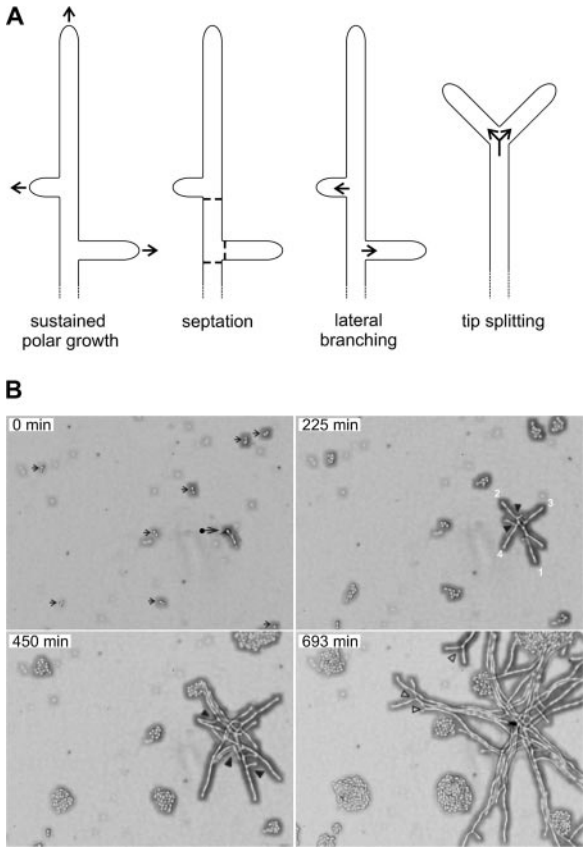

Figure 1. Differences in polar growth between *A. gossypii* and *S. cerevisiae*. (A) Schematic presentation of landmarks of hyphal growth of *A. gossypii*: Sustained polar growth (accelerating growth along a selected polarity-axis by continuous surface expansion at the tip), septation (growth of chitin-containing open rings at 30–50-μm distances at the cortex of hyphae and at the base of branches), lateral branching (successive selection of new axes of polarity at the cortex of elongating hyphae), and tip splitting (simultaneous generation of two new axes of polarity at fast growing tips). (B) Simultaneous monitoring of *A. gossypii* and *S. cerevisiae* growth. *A. gossypii* spores and *S. cerevisiae* cells were mixed and plated on AFM agar. After 4 h the agar surface was screened under the microscope. An area was selected for the start of the video (top left panel) showing eight *S. cerevisiae* cells after their first division (small arrows) and one germinated *A. gossypii* spore with the first emerged hypha (●). Growth in this area was monitored for 15 h at 25°C with pictures taken every 3 min (Supplementary Movie S1). After 225 min, the *S. cerevisiae* mini-colonies consist of four to eight cells, whereas the *A. gossypii* young mycelium has already developed nine extending hyphae. Two emerged, in addition to the first hypha, from the germinated spore and six originated from the initiation of lateral branches at the cortex of growing hyphae (two branches are marked by black arrow heads). At 450 min, the *S. cerevisiae* minicolonies have 12–32 cells and the *A. gossypii* young mycelium now consists of 23 hyphae due to 14 newly emerged lateral branches (black arrow heads). At 690 min the fastest hyphae, marked with open arrowheads, have started to symmetrically divide at their tips. Ten additional tip-splitting events were observed until the end of the movie at 897 min. The elongation speeds of the main hyphae during early mycelial development are ~10 μm/h (0 min), 15 μm/h (225 min), and 25 μm/h (450 min), as determined from the elongation of the four hyphae marked in frame 225 min, which were measured every four frames until 501 min. For technical reasons 21 frames were not recorded during the early period between the frames representing 132 and 135 min. To determine hyphal speeds at tip splitting hyphal elongations were measured during 18 frames before and after tip splitting. This mode of branching starts at elongation speeds of 80 μm/h. The highest speed observed at the end of Supplementary Movie S1 before a tip splitting was 140 μm/h. Four cases of consecutive tip splitting events were observed with an average distance of 190 μm and an average time interval of 140 min. Scale bar, 20 μm.

distinct functions in the cellular networks of both organisms. One example for shared and specific functions is *Ag*Spa2p, the first component identified in *A. gossypii* to permanently localize at hyphal tips, where it plays an essential role to reach maximal tip speeds (Knechtle *et al.*, 2003). These are properties specific for *A. gossypii*, because *Sc*Spa2p, the homolog in *S. cerevisiae*, does not localize permanently but only transiently to the bud tip and because a cellular process, controlling maximal bud tip speed, is unknown in morphogenesis of *S. cerevisiae* (Sheu *et al.*, 1998). Because *Sc*Spa2p is part of the polarisome, we speculated that *A. gossypii* homologues of other components of the polarisome complex, in particular the formin homology protein *Sc*Bni1p (Evangelista *et al.*, 2002; Sagot *et al.*, 2002a), could fulfill, in addition to common functions, also specific functions in sustained hyphal tip growth and tip splitting. Therefore, we searched for homologues in *A. gossypii* to *Sc*Bni1p and the related formin *Sc*Bnr1p and investigated to which degree the homologues would contribute to sustained hyphal tip growth and tip splitting.

The A. gossypii Formin Family Members

Using FASTA database searches (Pearson, 1990), we identified three formin homology members in the genome of *A. gossypii* (Dietrich *et al.*, 2004). By combining information from homology searches with synteny, these proteins can be categorized as follows: one syntenic homolog to the *S. cerevisiae BNI1* gene (*AFR669W*, in the following referred to as *AgBNI1*) and one syntenic and one nonsyntenic, telomere-located homolog to the *S. cerevisiae BNR1* gene (*AFR301C* and *AGL364C*, referred to as *AgBNR1* and *AgBNR2*, respectively). The formins *Sc*Bni1p and *Ag*Bni1p have almost the same size and domain composition (Figure 2A) using the domain definition from Evangelista *et al.* (2002). The two homologues to *Sc*Bnr1p differ much more in size and, interestingly, these size differences are located exclusively within the FH1 domains leading to differences in the number of short polyproline stretches (Figure 2B).

It was shown that the FH1 domain of formins can mediate interactions with profilin, an abundant actin-binding protein, thereby sequestering actin monomers (Pruyne *et al.*, 2002; Sagot *et al.*, 2002b; Moseley *et al.*, 2004). The FH2 domain provides the activity for nucleation of actin cables (Pruyne *et al.*, 2002; Sagot *et al.*, 2002a; Kovar *et al.*, 2003; Harris *et al.*, 2004; Moseley *et al.*, 2004). This domain is the most conserved and best characterized domain within formins and was used as a basis for the phylogenetic classification of over a hundred formins (Higgs and Peterson, 2005). The FH3 or Formin Homology 3 domain is only loosely conserved among formins and is defined by its role, in *S. cerevisiae*, to help locating *Sc*Bni1p to the bud tip (Ozaki-Kuroda *et al.*, 2001).

Other domains shown in Figure 2 are known to be involved in diverse protein interactions in *S. cerevisiae*. The Spa2-binding domain (SBD) and to a lesser degree the Bud6-binding domain (BBD) are important for localization of ScBni1p to the growing bud tip (Ozaki-Kuroda *et al.*, 2001; Sagot *et al.*, 2002a). The Rho-binding domain (RBD) interacts with small GTPases of the Rho-type and also undergoes an intramolecular association with a short carboxy-terminal domain called diaphanous autoregulatory domain (DAD). This association, indicated by the arrow in Figure 2A, prevents actin cable assembly unless an activated GTPase binds to this domain (Alberts, 2001). A short sequence similar to the known functional DAD residues of *Sc*Bni1p is also found in all members of the Bnr1 group (small black bars in Figure 2B) but its function remains unclear. Importantly, in contrast to *Sc*Bnr1p, am RBD could not be identified in the *A. gossypii*

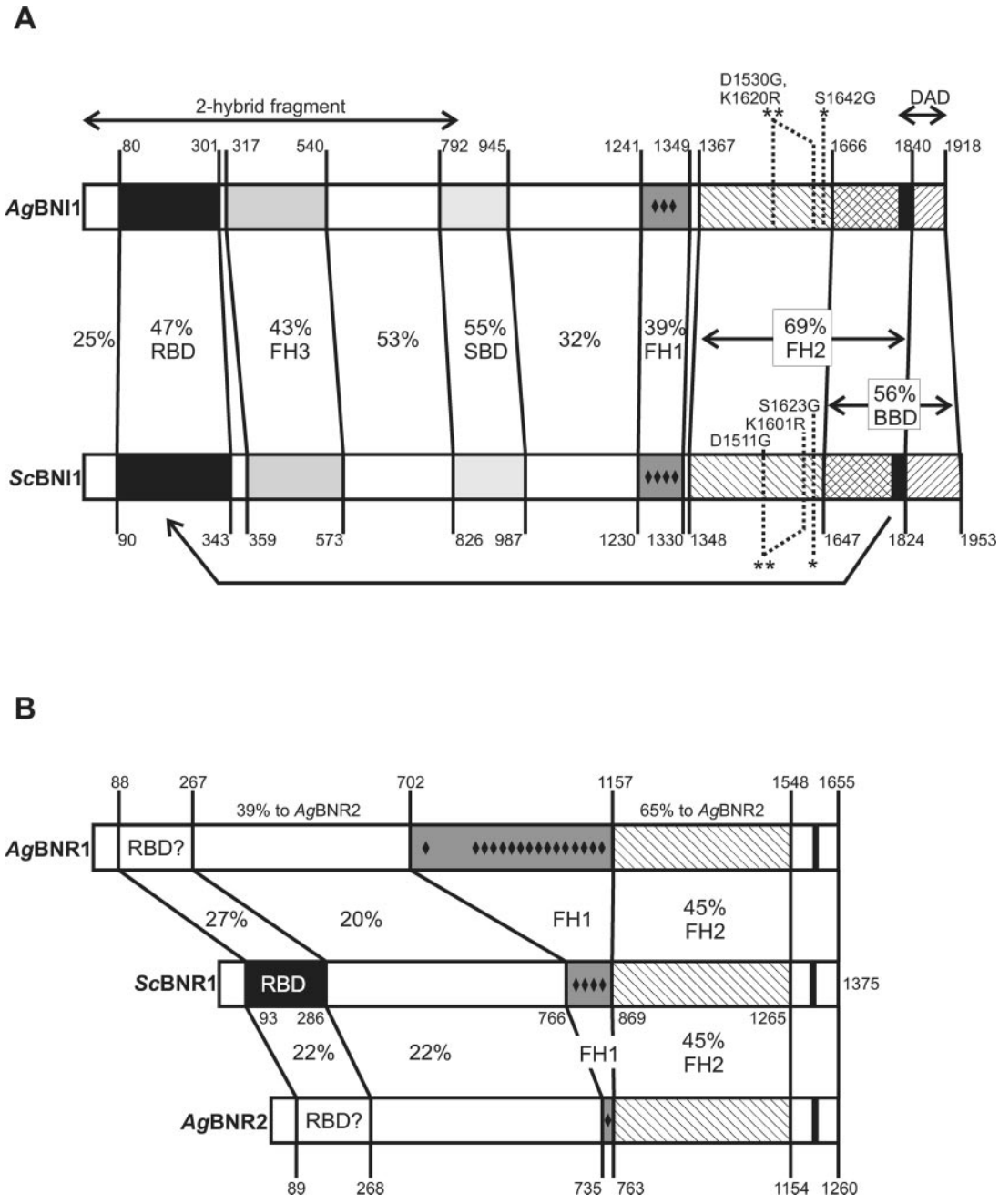

Figure 2. Domain comparisons between formin homologues of *S. cerevisiae* and *A. gossypii.* (A) Comparison of *Ag*Bni1p and *Sc*Bni1p. The domain structure of *Sc*Bni1p is based on the one published by Evangelista *et al.* (2002). Domain borders were first determined using the gap program of the GCG Wisconsin Package (Accelrys), which uses an Needleman-Wunsch algorithm (Needleman and Wunsch, 1970). Each domain was realigned and the identity values were taken from the output. All distances are drawn to a relative scale. RBD, Rho-binding domain; FH1–3, Formin Homology domain 1–3; SPD, Spa2-binding domain; BBD, Bud6-binding domain; DAD, diaphanous autoregulatory domain, which is drawn as black bar within BBD. The point mutations and the DAD deletion used in this work are indicated as well as the boundaries of the amino-terminal fragment used in two-hybrid studies. (B) Comparison of *Ag*Bnr1p and *Ag*Bnr2p with *Sc*Bnr1p. The domain structure of *Sc*Bnr1p is based on that of *Sc*Bni1p. Domain borders were determined and marked as described in A. No clear indication of an RBD was found in the two *A. gossypii* homologues. Small black diamonds indicate positions of short stretches of two or more prolines that are not separated by more than one other residue.

homologues searching for this domain (DRF_GBD) in PFAM version 17.0. This result is consistent with our finding that neither full-length nor amino-terminal parts of *Ag*Bnr1p and *Ag*Bnr2p bind to wild-type or activated forms of all *A. gossypii* Rho-GTPases in a two-hybrid test (unpublished data).

Because the two *S. cerevisiae* formins have partially overlapping functions allowing, for example, single deletions to grow, we expected, based on the domain comparisons, also to find overlapping functions in the three formins of *A. gossypii*.

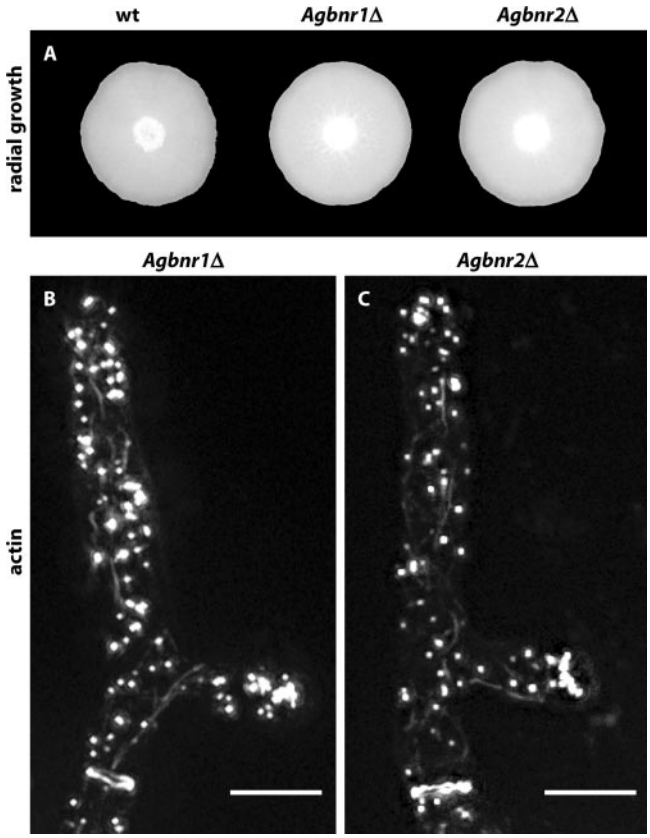

Figure 3. Wild type-like growth of *Agbnr1* and *Agbnr2* deletions. (A) Mycelial colonies from *A. gossypii* wild-type and single deletion strains. Small aliquots of mycelia were transferred to the middle of full medium plates and grown for 6 d at 30°C. Bar, 1.0 cm. (B and C) Visualization of actin patches, actin cables, and actin rings by staining young mycelium of the respective deletion strains with Alexa-phalloidin (Knechtle *et al.,* 2003). In both panels a growing tip is at the top and an actin ring is seen at the bottom below an emerged lateral branch. Bars, 5 μm.

Single Deletions of Agbnr1 and Agbnr2 Are Viable But Not the Double Deletion

To investigate the cellular function of the two homologues of *Sc*Bnr1p, we first deleted the entire ORFs of *AgBNR1* and *AgBNR2* by PCR-based gene targeting using a cassette coding for resistance against geneticin (G418). Young mycelium with 20–40 nuclei was transformed to geneticin-resistance. These primary transformants are heterokaryotic because their haploid nuclei carry either the wild-type or the deletion allele. Homokaryotic deletion transformants were obtained from spores that contain single nuclei and that were dissected on selective agar medium. Growing homokaryotic transformants were rechecked for the loss of the wild-type and presence of the deletion allele and were phenotypically characterized.

As can be seen in Figure 3A, the mycelial development of both single deletions is not perturbed. Consistent with this wild type-like growth, all actin structures can be observed by Alexa-phalloidin staining as shown in Figure 3, B and C. Staining with calcofluor white revealed an increased number of incomplete chitin rings in the *Agbnr2* deletion, and a fusion with GFP revealed that at least a fraction of the *Ag*Bnr2p-GFP proteins locates at septa, whereas no fluorescence was detected at the tips (unpublished data). Several attempts to locate an *Ag*Bnr1-GFP fusion remained unsuccessful.

The viability of both deletions indicates that the two *Ag*Bnrp homologues probably encode overlapping functions. The genomic arrangement of the *A. gossypii BNR* genes indeed suggests that *AgBNR2* most likely originates from a duplication of an ancient *AgBNR1* gene involving transposition of one copy to the telomere region of chromosome VI. We therefore constructed and tested double deletions of both homologues. Because of the lack of a functional mating system in *A. gossypii,* we had to delete the *AgBNR2* gene in a strain already deleted for the *AgBNR1* gene. This resulted in transformants that are homokaryotic for the *Agbnr1* deletion (ClonNAT resistance marker) and heterokaryotic for the *Agbnr2* deletion (geneticin resistance marker). PCR-verified heterokaryotic transformants were sporulated and spores were dissected on different selection media. Spores were viable on ClonNAT, selecting for the *Agbnr1* deletion, but nonviable on geneticin, selecting for the *Agbnr1*/*Agbnr2* double deletion ($n > 100$). To avoid the possibility that the *Agbnr1* deletion strain used to construct the double deletion carried an unknown mutation, which is colethal with the introduced *Agbnr2* deletion, we repeated the experiment with a newly constructed *Agbnr1* transformant as the recipient strain, now marked by geneticin resistance. Then we used leucine auxotrophy as selection for the *Agbnr2* deletion. Again, we were unable to isolate any mature mycelium carrying a homokaryotic *Agbnr1/Agbnr2* double deletion. To see if the nonviable spores showed residual growth, we looked for germination structures under the microscope. None of the spores formed a germ bubble ($n > 100$), indicating a common function of *Ag*Bnr1p and *Ag*Bnr2p essential very early in germination.

Deletion of AgBNI1 Is Lethal

To investigate the functions of *AgBNI1,* we first deleted the entire ORF. More than 100 spores obtained from the primary heterokaryotic mycelium were dissected and placed on selective medium. None of these spores gave rise to a mature mycelium. Thus, deletion of *AgBNI1* is lethal despite the presence of the two other formin genes, *AgBNR1* and *AgBNR2,* indicating an essential role of the formin *Ag*Bni1p. In *S. cerevisiae*, mutants with deletions of either one of the two formin genes, *ScBNI1* and *ScBNR1*, are viable and only deletion of both genes is lethal (Imamura *et al.,* 1997).

Microscopic observation of *Agbni1*Δ (Figure 4) revealed that spores started swelling like wild type, but were not able to initiate hyphal growth. Instead, irregular isotropic growth proceeded for at least 20 h, generating giant, potatolike cells containing over 100 nuclei. Because formins were reported to catalyze actin cable polymerization (Pruyne *et al.,* 2002; Sagot *et al.,* 2002b), we investigated the actin cytoskeleton of *Agbni1*Δ stained with Alexa-phalloidin. Long, polarized actin cables, reaching the tips, have been reported for *A. gossypii* wild type (Knechtle *et al.* (2003) and Figure 4D). The images in Figure 4, E and F, show that *Agbni1* deletion mutants do not contain polarized actin cables and that actin patches are distributed all over the cell cortex. This is in contrast to wild-type hyphae, where patches are concentrated at the tips The only concentration of actin patches is observed along structures which, according to the DIC images in Figure 4, B and C, most likely mark sites of septum formation as described before (Knechtle *et al.,* 2003). Thus, *AgBNI1* might not be essential for septum formation but is required for actin cable formation and hyphal morphology.

The loss of actin cable formation in the *Agbni1* deletion raises an important question. Why is this loss not compen-

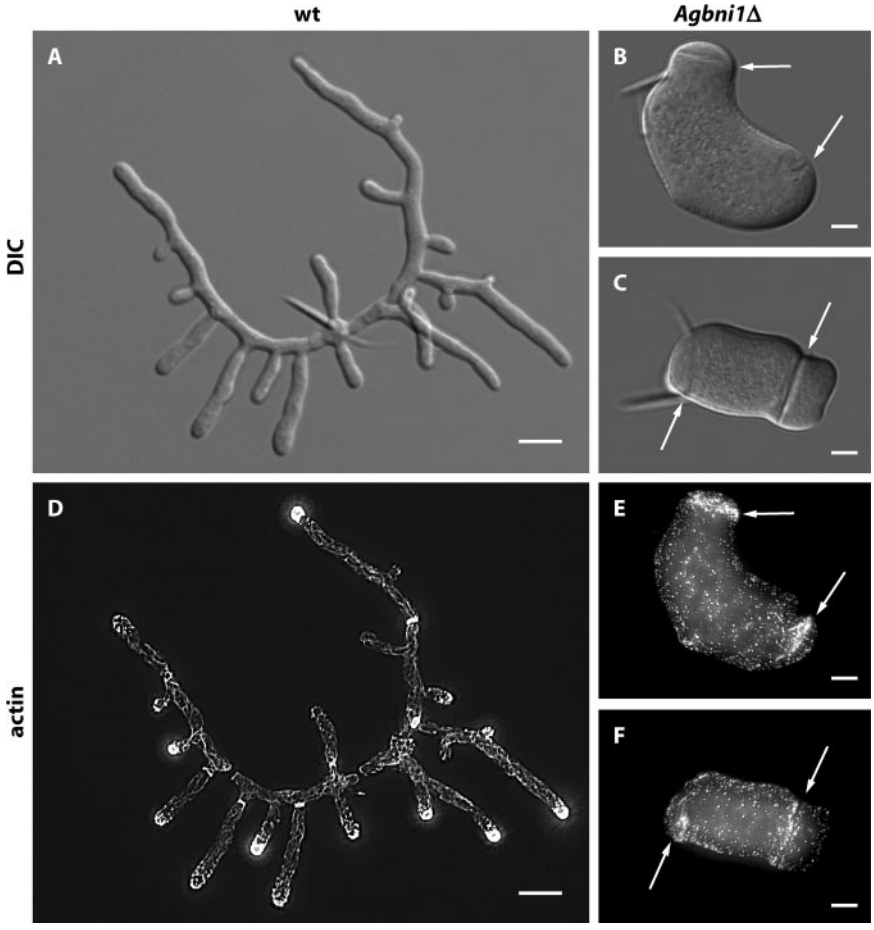

Figure 4. Lack of mycelial development after deletion of the single formin gene *AgBNI1.* Spores from wild type and from heterokaryotic *Agbni1*Δ transformants were grown over night at 30°C in AFM and AFM-Geneticin medium, respectively. DIC images are shown for wild-type (A) and *Agbni1*Δ (B and C), and fluorescence images for rhodamine-stained wild-type (D) and Alexa-phalloidin-stained *Agbni1*Δ (E and F). Arrows mark giant septumlike structures in *Agbni1*Δ that are visible by DIC and by actin staining. The needlelike structures attached to the middle of the young mycelium (A) and to one pole of the giant cells (B and C) originate from the spores, which have the shape of ~20-μm-long needles. Bars, (A and D) 10 μm and 5 μm for all other images.

sated, as in *S. cerevisiae*, by one of the two other formin homology members? The domain comparisons of Figure 2 do not reveal an answer because there is no significant difference between formin homologues of both organisms with respect to the domains responsible for actin cable formation. Therefore we hypothesized that *Ag*Bni1p is essential because its essential function may be connected to its location.

AgBni1p Locates to Hyphal Tips

To determine the location of *Ag*Bni1p, we constructed a GFP fusion at the genomic locus of *AgBNI1* and first tested whether the fusion protein is functional. Spores expressing *Ag*Bni1p-GFP developed to a young mycelium with actin cables, actin patches, and actin rings indistinguishable from wild type. Mature hyphae displayed regular tip splitting, only their maximal elongation speed was slightly slower than wild type (unpublished data). Microscopic images revealed a very weak GFP signal, always located at the tip of hyphae, which was detectable in both, young mycelium (Figure 5A) and mature hyphae (Figure 5B). Interestingly, no signal could be detected at sites of septation in over hundred apical regions inspected. This is in contrast to *S. cerevisiae* where Bni1p-GFP localizes, in addition to polarized bud tips, also as ringlike structures at sites of septation (Ozaki-Kuroda *et al.,* 2001), where it is most likely involved in cell separation, a process that does not occur in growing *A. gossypii* hyphae. Therefore the observed localization is consistent with an exclusive role for *Ag*Bni1p in tip growth.

Localization of the Polarisome Component AgSpa2p in the Agbni1Δ Mutant

One possible essential process *Ag*Bni1p that could be involved in at hyphal tips is the assembly or stabilization of a polarisome-like structure, which acts as a polarity control complex. For example, Bauer *et al.* (2004) could recently demonstrate that the GTPase *Ag*Bud1p is important to stably maintain the polarisome marker *Ag*Spa2p-GFP at hyphal tips and that transient loss of this tip marker in an *Agbud1* deletion causes an immediate arrest of polar growth. To test a possible essential role for *Ag*Bni1p in the assembly or stabilization of the "polarisome complex," we deleted *AgBNI1* in a strain expressing GFP-labeled *Ag*Spa2p. *Ag*Spa2p permanently localizes to the tips of elongating hyphae (Knechtle *et al.,* 2003). In the giant *Agbni1*Δ cells *Ag*Spa2p-GFP is always found at the cortex of the slowly expanding zone opposite from the spore needle (Figure 5C), indicating that *Ag*Bni1p does not play an essential role in polarizing *Ag*Spa2p. The observed polarization may be the reason why giant *Agbni1*Δ cells form potato-shaped structures instead of large round cells, like mutants of *Agcdc24* and *Agcdc42,* which are blocked in early steps of polarity establishment (Wendland and Philippsen, 2001).

Mutation of a Single Amino Acid in the FH2 Domain of AgBni1p Is Lethal

The experiments presented so far and the domain comparison of Bni1p from *A. gossypii* and *S. cerevisiae* discussed in Figure 2 suggest similar molecular properties of both pro-

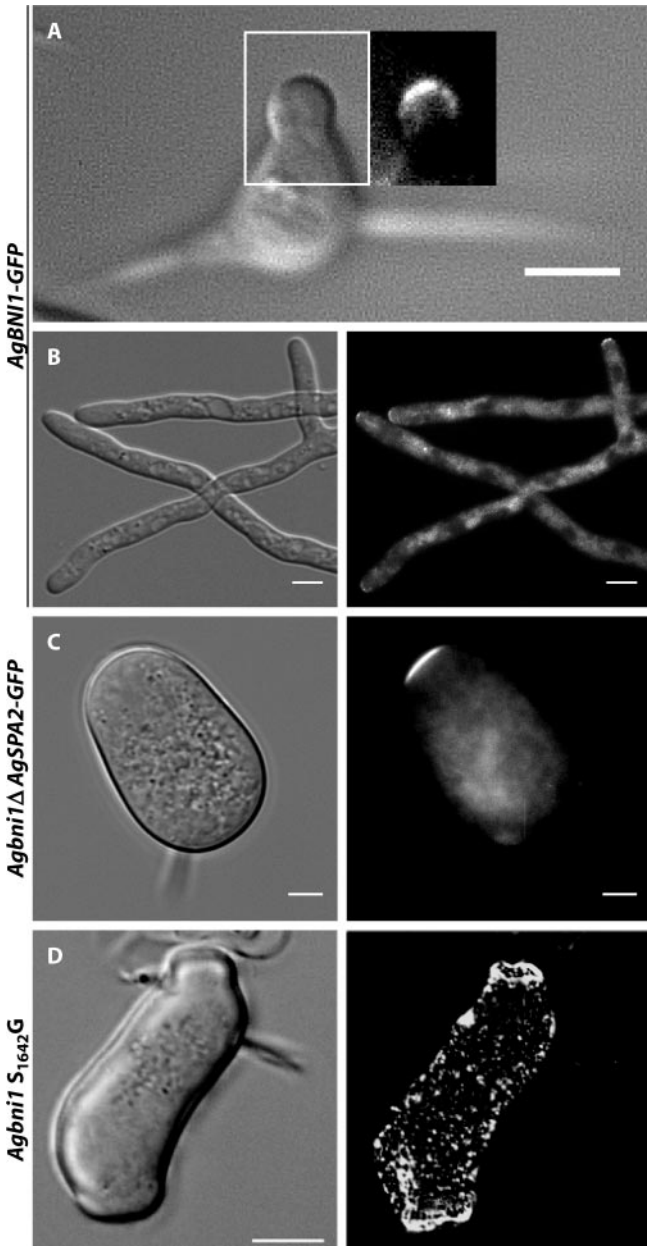

Figure 5. Localization of *Ag*Bni1p-GFP at hyphal tips. (A) Brightfield and fluorescence image of an *A. gossypii* germling carrying one copy of *AgBNI1-GFP* expressed from the endogenous *BNI1* promoter. Because of high autofluorescence of spores, the fluorescence image is only shown for the area corresponding to the white rectangle. Scale bar, 5 μm. (B) Brightfield and fluorescence image of a mature hypha expressing *Ag*Bni1p-GFP from a genomic fusion gene. Scale bar, 5 μm. (C) Localization of *Ag*Spa2p-GFP in *Agbni1*Δ. DIC image and fluorescence images of *Agbni1*Δ cells carrying a *SPA2-GFP* fusion at the *AgSPA2* locus. Spores from heterokaryotic transformants were grown in AFM-Geneticin medium over night at 30°C. Scale bar, 5 μm. (D) Phenotype of the single $S_{1642}G$ substitution in the FH2 domain of *Ag*Bni1p. Spores from heterokaryotic transformants were grown over night in liquid AFM-Geneticin medium at 30°C and stained for actin with Alexa phalloidin. The fluorescence image (top) and the DIC image (bottom) were taken from the same cell. Scale bar, 10 μm.

teins. One important property of *Ag*Bni1p and *Sc*Bni1p is the nucleation of actin cables, which resides within the FH2 domain. We asked whether the characteristic phenotype of the *AgBNI1* deletion is only due to a tip-located loss of actin polymerization capability and subsequent loss of actin cables rather than loss of other functions. To test this, we constructed point mutations in the FH2 domain of *Ag*Bni1p, leading to the amino acid substitutions $S_{1642}G$ in one and $D_{1530}G$, $K_{1620}R$ in a second mutant. Especially the residues mutated in the second mutant are highly conserved throughout all formin proteins (Higgs and Peterson, 2005). In *S. cerevisiae*, both homologous substitutions $S_{1623}G$ and $D_{1511}G$, $K_{1601}R$ lead to temperature-sensitive strains in a background deleted for *ScBNR1,* the second formin gene (Evangelista *et al.,* 2002). We expected to find temperature-sensitive phenotypes for both *A. gossypii* mutants. Surprisingly, the analogous substitutions in *Ag*Bni1p were lethal, even at 16°C. Like the complete deletion, these point mutants were able to form giant cells with many actin patches but without actin cables (Figure 5D). These experiments indicate that the tip-located assembly of actin cables represents the essential function of the *Ag*Bni1p formin, which emphasizes the importance of actin cables for hyphal growth.

Actin Cable-based Vesicle Transport Is Defect in Agbni1D

The loss of actin cables should severely impede delivery of secretory vesicles to hyphal tips. To confirm that *Ag*Bni1p is needed for secretory vesicle transport, we isolated the *AgSEC4* gene by homology to the *S. cerevisiae SEC4* gene and constructed a GFP-fusion. In budding yeast, a GFP-Sec4p fusion protein localizes to secretory vesicles and moves in a directed manner along actin cables toward the bud tip (Schott *et al.,* 2002). We transformed *A. gossypii* with a plasmid expressing an amino-terminal GFP-*Ag*Sec4p fusion under control of the native *AgSEC4* promoter. As shown in Figure 6A, the fusion product localizes mainly to the tip. Addition of latrunculin A, which disrupts actin structures, abolishes vesicular movement and apical localization, giving rise to a uniform fluorescence within hyphae (Figure 6B). To observe the localization of vesicles in the absence of *Ag*Bni1p, we transformed a heterokaryotic *Agbni1*Δ mycelium with the plasmid expressing the GFP-*Ag*Sec4p fusion protein. Spores of these transformants were grown under conditions selective for both, the *Agbni1* deletion and the plasmid. In all growing giant cells the GFP fluorescence was evenly distributed (Figure 6C). This verifies that continuous tip-directed transport of secretory vesicles via actin cables is essential for hyphal growth.

Hyphal Morphogenesis in the Presence of Constitutively Active AgBni1p (AgBNI1ΔD)

We wanted to know whether an overactivation of the *Ag*Bni1 protein would increase hyphal elongation rates. We speculated that such a mutant should assemble more actin cables emanating from the tips, thus enhancing the transport rate of secretory vesicles toward the tip. To test this hypothesis, we deleted in *AgBNI1* the coding sequence of the carboxy-terminal DAD (see Figure 2), thereby eliminating in the expressed protein the inactivating interaction of the DAD domain with the amino terminus.

Several independent mutants were isolated. All show a complete change in branching pattern. Although morphogenesis of young wild-type mycelium exclusively displays lateral branching (Figure 7, A–C), the overactivation of the *Ag*Bni1p formin suppresses this branching mode and induces successive and symmetric hyphal splitting at tips (Figure 7, D–F). Lateral branching events occur only late and very rarely in this mutant, as concluded from videomicroscopy of 10 developing young mycelia. Examples are docu-

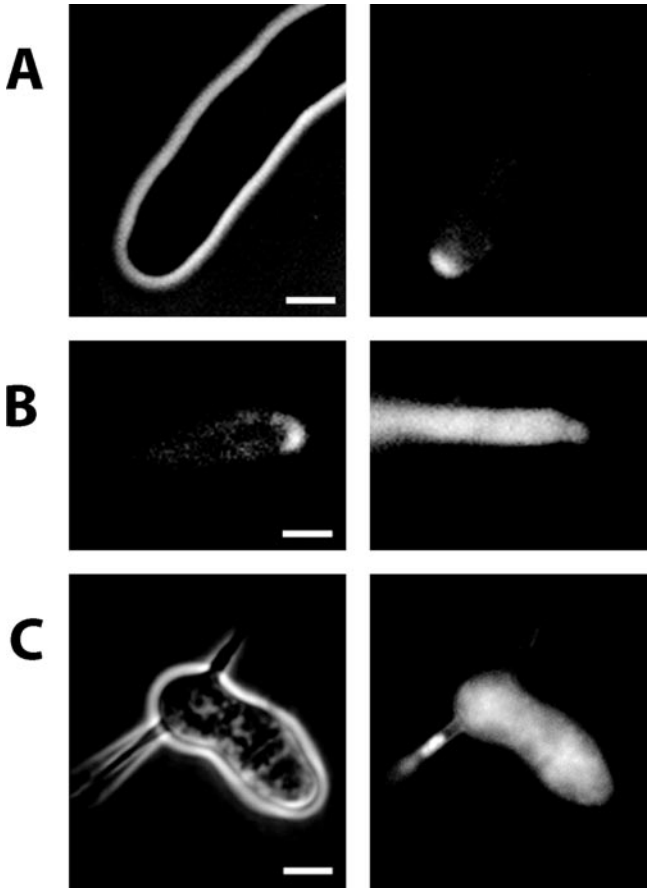

Figure 6. Distribution of GFP-Sec4p in wild type and *Agbni1*Δ. (A) Brightfield (left) and GFP-fluorescence (right) micrographs of a single wild-type hypha carrying a GFP-SEC4 fusion. The main fluorescence localizes to the tip. (B) Localization of GFP-Sec4p prior (left) and after (right) treatment with 200 μM latrunculin A for 1.5 min. (C) Brightfield (left) and GFP-fluorescence (right) images of *Agbni1*Δ carrying a *GFP-SEC4* fusion gene. All strains were grown in liquid selective medium at 30°C over night. Scale bars, 5 μm.

mented in Supplementary Movies S2-S4 for wild type and Supplementary Movies S5-S7 for *AgBNI1*Δ*D* (see Supplementary Material).

Quantitative evaluation of the movies reveals similar initial tip extension speeds for wild type and *AgBNI1*Δ*D* (Figure 8A). However, the average diameter of young hyphae of the mutant has almost doubled compared with wild type based on 300 measurements of three hyphae each (4.63 ± 0.46 μm for wild type and 7.52 ± 1.1 μm for mutant hyphae). These parameters allowed us to calculate for each time point the surface expansion rate, which, during the first 4 h, is up to three times higher in the mutant compared with wild type (Figure 8B). This increase in surface growth strongly indicates that an overactivation of *Ag*Bni1p can enhance the traffic of tip-directed secretory vesicles. This idea is supported by three experimental results. First, constitutively activated *Ag*Bni1ΔD proteins still locate to the tips (20/20) of hyphae (Figure 8C). Second, a two to three times higher number of actin cables can be observed in the apical region of mutant hyphae (Figure 8D) compared with wild-type hyphae (Figure 8E). And third, more vesicles are transported to the tip region as evident from the larger area of accumulated secretory vesicles in mutant hyphae (Figure 8, F and G) compared with wild-type hyphae (Figure 6A).

The nonregulatable, overactive *Ag*Bni1ΔD formin leads to a growth advantage during the early mycelial development but has a negative effect on the further development to a fast spreading colony (Figure 8H). Already after 6 to 7 h the elongation rate of mutant hyphae and with that the surface expansion rate reaches a plateau, whereas the elongation of wild-type hyphae continues to accelerate (Figure 8, A and B). This difference in growth rates may be due to the high frequency of premature tip splitting events in the mutant, which impedes hyphal speed acceleration and thus leads to a slower growing mycelium compared with wild type.

AgBni1p Is an Effector of AgCdc42p

The domain composition of *Ag*Bni1p predicts that it is activated when a GTP-bound Rho-type GTPase interacts with the amino-terminal RBD (Figure 2). We searched for candidates of such activator among *A. gossypii* homologues of Rho-type GTPases using two criteria: Its GTP-bound form should interact with the amino-terminus of *Ag*Bni1p, and a GTP-locked form of this protein should induce tip splitting in young hyphae due to a permanent activation of *Ag*Bni1p, similarly as observed for young hyphae of the *AgBNI1*Δ*D* mutant. By systematic two-hybrid analysis of the *Ag*Bni1p amino-terminus against all *A. gossypii* Rho-type GTPases and by videomicroscopy of GTP-locked mutants of the three Rho-type GTPases, which scored positive in the first test, we identified *Ag*Cdc42p as the only candidate. The two-hybrid result is summarized in Figure 9A and two microscopic images showing tip splitting in young hyphae expressing GTP-locked *Ag*Cdc42p are presented in Figure 9B. These hyphae carry only the mutated *AgCDC42* allele and show growth defects preventing the young mycelia from further development. This is most likely due the multitude of effector proteins that are regulated by *Ag*Cdc42p.

DISCUSSION

The filamentous fungus *A. gossypii* and the budding yeast *S. cerevisiae* have different life styles (see Supplementary Movie S1) despite very similar gene contents and conserved domain compositions of gene products (Dietrich *et al.*, 2004). Both organisms can establish polar growth but in *S. cerevisiae* periods of growth alternate with cell divisions, whereas *A. gossypii* cells (hyphae) grow for unlimited periods without undergoing divisions. In addition, *A. gossypii* hyphae can establish multiple new axes of polarity, e.g., during lateral branching or tip splitting. In contrast, wild-type yeast cells never form more than one new bud at the same time (Caviston *et al.*, 2002). We describe here a role for the *Ag*Bni1p formin in two of these processes: the establishment of polarity (formation of hyphae) and the controlled division of one axis of polarity into two new polarity axes (tip splitting), a novel function for this protein class.

Redundance of Formins in A. gossypii

The lethality of the *Agbni1* deletion was surprising because *A. gossypii* contains two additional formin genes, *AgBNR1* and *AgBNR2*, and because all three formin genes encode proteins with similar domains, notably the actin nucleation domain FH2. The deletion of either one of the *Ag*BNR genes is fully viable indicating overlapping functions in the *Ag*Bnr formins. These results made us at first conclude that the lethality of *Agbni1*Δ is due to distinct functions of members of the *Ag*Bni1p and the *Ag*Bnr proteins. This idea was supported by comparison to the more distantly related fission yeast *S. pombe*, which expresses three members of the formin family with clear separation of functions. For3 is involved in

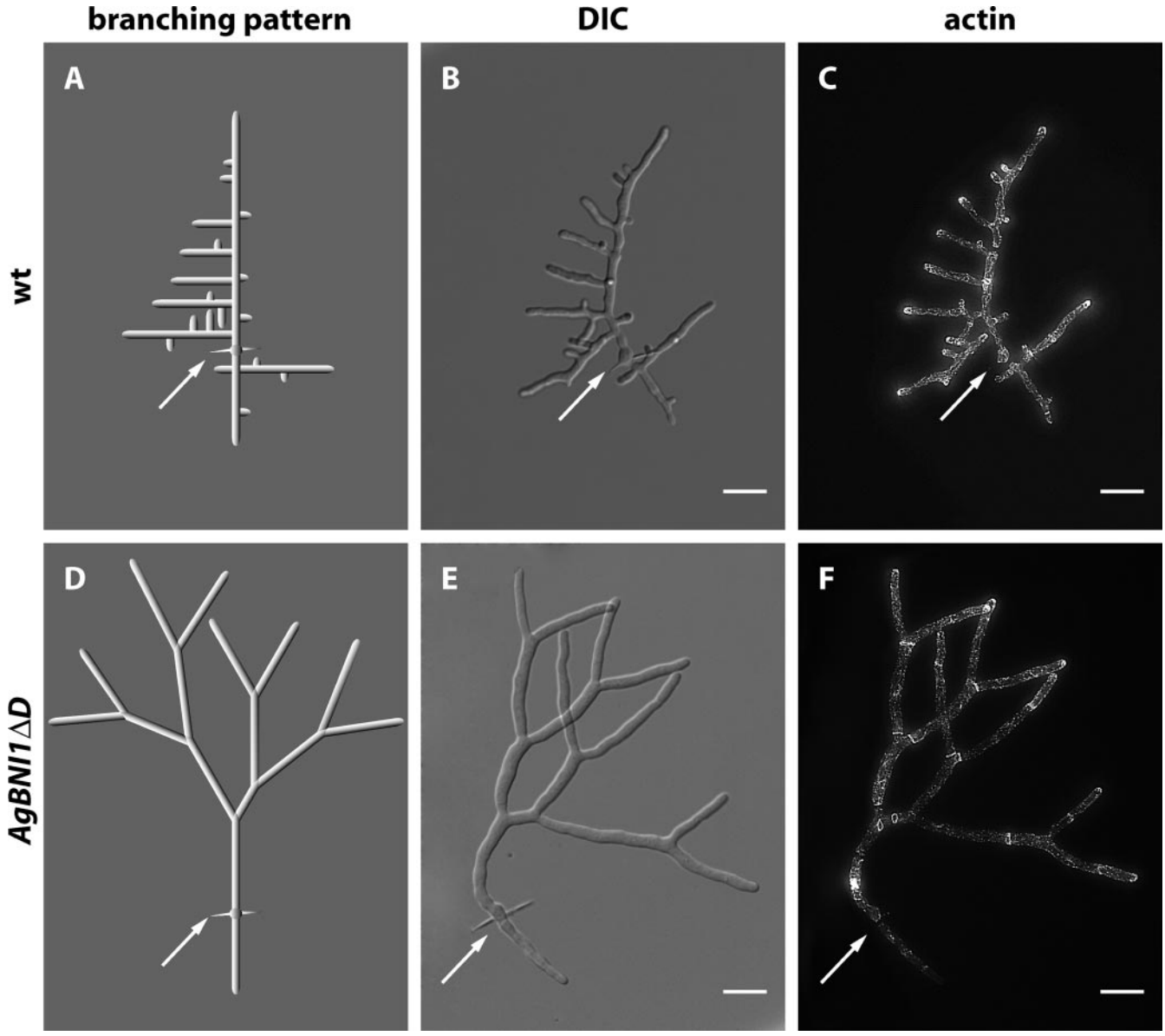

Figure 7. Altered morphogenesis of *AgBNI1ΔD* mycelium. Wild-type and *AgBNI1ΔD* spores were incubated in liquid AFM medium at 30°C. After 18 h aliquots were stained with Alexa-phalloidin and mounted for microscopy. (A) Idealized branching scheme of the young wild-type mycelium shown as DIC image in B and as fluorescence image in C. The white arrows mark the needle of the spore from which two main hyphae developed in opposite directions. New branches always emerged distant from the tip and in an about right angle from the polarity-axis of the main hyphae, leading to a typical "Christmas tree" appearance. (D) Idealized tip splitting pattern of the young *AgBNI1ΔD* mycelium shown as DIC image in E and as fluorescence image in F. The white arrows mark the original position of the spore. Scale bar, 10 μm.

cell polarity (Feierbach and Chang, 2001), Cdc12 is involved in cytokinesis (Chang *et al.*, 1997) and Fus1 is necessary for cell fusion during mating (Petersen *et al.*, 1998a). Although *S. pombe for3Δ* had no visible actin cables (Feierbach and Chang, 2001) or the cables were shorter in size and reduced in number (Nakano *et al.*, 2002), cells were still able to grow in a polarized manner unlike a deletion of *Agbni1*.

Different functions were also described for the baker's yeast formins *Sc*Bni1p and *Sc*Bnr1p (Pruyne *et al.*, 2004). *Sc*Bni1p localizes mainly to the bud tip where it forms actin cables. It is also found at the septum in a very late phase of bud formation, when the direction of growth polarity has already switched. *Sc*Bnr1p in contrast localizes exclusively and already during early phases of bud formation to the forming septum. However, budding yeast cells can still survive in the absence of *Sc*Bni1p because the septum-associated *Sc*Bnr1p is also able to nucleate actin cables, thereby providing the close-by growing bud with secretory vesicles. This short distance between the septum and the growing bud tip, e.g., during axial budding, is probably of key importance for the viability of cells lacking the *Sc*Bni1p formin. At increasing distances between the septum and the growing tip, formin deletion experiments may give different results. For example, assuming similar actin nucleating functions for the formins in *A. gossypii* but distinct protein localization requirements, the lethality of the *Agbni1* dele-

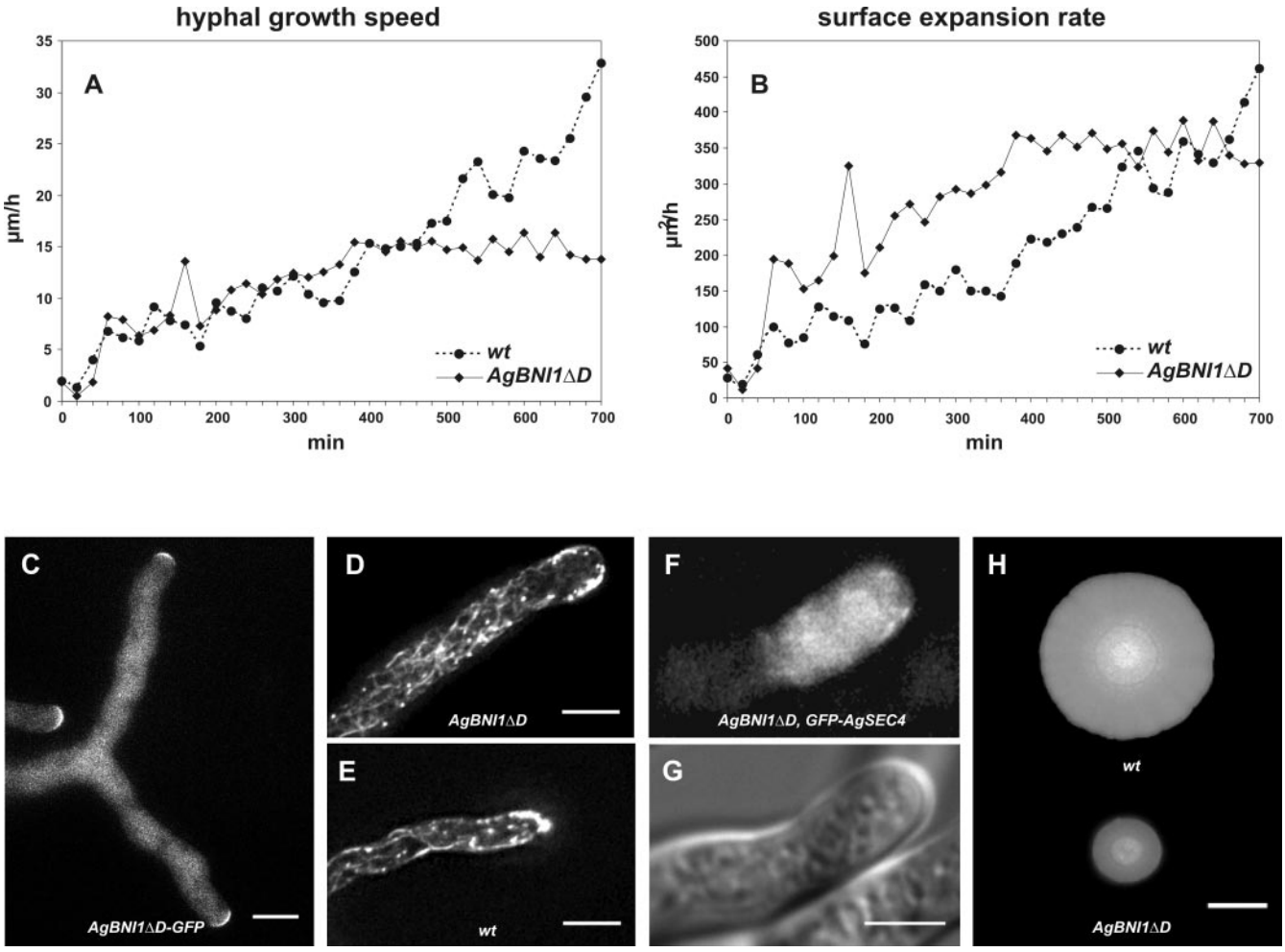

Figure 8. Increase in surface expansion and number of actin cables in *AgBNI1ΔD*. (A) Elongation speeds in μm/h of wild-type hyphae (●) and *AgBNI1ΔD* hyphae (♦) during the first 700 min of hyphal development. The data points represent the average from two hyphae followed in three young mycelia each, starting shortly after the first hypha has emerged from a germinated spore. (B) Surface expansion rates at hyphal tips of wild type (●) and *AgBNI1ΔD* (♦) were calculated from the elongation speeds determined in A, and the hyphal diameters were measured every 10 μm. (C) Localization of *Ag*Bni1ΔD-GFP fusion proteins at hyphal tips. (D) Visualization by epifluorescence microscopy of rhodamine-phalloidin-stained F-actin in *AgBNI1ΔD*. For several hyphae a stack of 16 planes taken at 0.4-μm distances was analyzed. Because of the high density of actin cables along the cortex only a maximum projection of the top third of the hypha (three planes) is shown. Four to five actin cables can be seen per cross section, which represents about one-third of the density of cortical actin cables in the hypha. (E) Rhodamine-phalloidin stained F-actin in wild-type *A. gossypii*. The stack of 16 planes was processed as described for D, and only the top third of the hypha is shown. Only one to two cortical actin cables can be seen per cross section. (F and G) Visualization of GFP-*Ag*SEC4-labeled vesicles in the tip region of an *AgBNI1ΔD* hypha and the corresponding DIC image. (H) Mycelial colonies of wild type and *AgBNI1ΔD* after growth on AFM agar at 30°C for 5 d. Bars, (C–F) 5 μm, (H) 2 cm.

tion could be explained by the large distance between the growing tip and the nearest septum, preventing septum-associated formin functions to complement the loss of such functions at hyphal tips. This alternative interpretation is supported by the fact that we were able to visualize *Ag*Bni1p-GFP at hyphal tips, but not at septa, and *Ag*Bnr2p-GFP at septa but not at hyphal tips.

The fact that *Ag*Bni1p functions in hyphal emergence and elongation, but probably not in septum formation, indicates that it is also functionally different from SepA, the only other formin described in a filamentous fungus so far. SepA from *Aspergillus nidulans* localizes to the tip of hyphae and to septa, and it is essential for morphogenesis. Interestingly, some SepA mutants, defective in septum formation, are still able to form hyphae (Sharpless and Harris, 2002). Therefore, mutant formins can probably still induce actin cables at hyphal tips, or another, so far unidentified formin gene, is present in the genome of *A. nidulans*.

AgBni1p and the Actin Cytoskeleton

The phenotype observed for the *AgBNI1* deletion, lack of actin cables and hyphal growth, indicated that an important function of *Ag*Bni1p might be the regulation of vesicle transport via actin cables. *A. gossypii* hyphae are capable to grow with very high growth speeds of up to 170 μm/h (Knechtle *et al.*, 2003). This speed obviously requires a constant and very efficient transport of growth material toward the elongating tips. Our results show that single amino acid changes in the FH2 domain of *Ag*Bni1p, which is responsible for actin cable assembly, can only expand to potato-shaped cells,

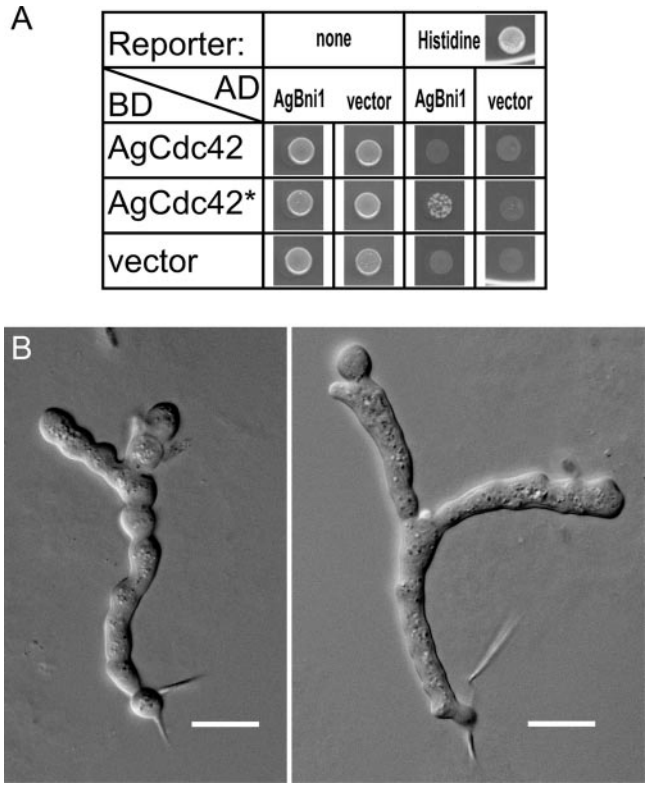

Figure 9. *Ag*Cdc42p regulates tip splitting. (A) Two-hybrid assay of *Ag*Cdc42p-GTP and the amino-terminal half of *Ag*Bni1p. Each spot corresponds to 5 μl of a yeast culture of strain *PJ69–4a* with an OD_{600} of 1, transformed with plasmids encoding fusions of the indicated proteins to either the Gal4-activation domain (AD) or to the Gal4-DNA-binding domain (BD) or, as control, transformed with the vector plasmid. The cells were spotted on a medium allowing to select for the plasmids and were grown overnight at 30°C to screen for protein-protein interactions by growth in the absence of histidine. (B) Altered morphogenesis of *A. gossypii* expressing GTP-locked *Ag*Cdc42p. A heterokaryotic strain of *A. gossypii* was constructed carrying the point mutation *AgCdc42*-Q_{61}H that encodes a protein mimicking the GTP-bound and therefore activated state of the GTPase. Spores were dissected by micromanipulation and allowed to germinate under conditions selecting only for spores carrying the GTP-locked *AgCDC42* allele. The two microscopic images show examples of tip splitting soon after the first hypha emerged from the germling. These hyphae carry only the mutated *AgCDC42* allele and show growth defects preventing the young mycelia from further development. This is most likely due the multitude of effector proteins that are regulated by *Ag*Cdc42p. Scale bar, 10 μm.

which lack polarized actin cables like the deletion mutant. Therefore, it might be the defect of actin cable-based transport, which leads to the phenotype observed when *AgBNI1* is deleted. It is known from several studies, that actin cables can serve as tracks for different cargos such as secretory vesicles (Johnston *et al.*, 1991) and several organelles (Simon *et al.*, 1995; Hill *et al.*, 1996; Hoepfner *et al.*, 2001; Rossanese *et al.*, 2001) as well as mRNA (Bobola *et al.*, 1996; Sil and Herskowitz, 1996; Takizawa *et al.*, 2000). Using the *Ag*Sec4p fused to GFP, we were able to show that secretory vesicles use actin cables for accumulation at the hyphal tips. They no longer do so in *AgBNI1*-deleted hyphae even though the polarisome component *Ag*Spa2p localizes correctly to the cortex at the slowly expanding growth zone, which explains the potatolike shape of the giant mutant cells.

Regulation of Tip Splitting by AgBni1p

Tip splitting, the symmetric division of the polar growth zone of a single growing cell, is to our knowledge limited to filamentous fungi and to dendrites of neuronal cells. Hyphae of *A. gossypii* usually start tip splitting under optimal conditions 12–14 h after the first hyphae emerged from germinated spores (Ayad-Durieux *et al.*, 2000). Premature tip splitting, already after 6–8 h of elongation and before any lateral branching, as found for the constitutively active *Ag*Bni1p protein, was not described before. In an *Agcla4* deletion strain, premature tip splitting was previously observed but after normal development of a young mycelium, including lateral branching (Ayad-Durieux *et al.*, 2000). *Ag*Cla4p is a homologue of the PAK21 kinase Cla4p from *S. cerevisiae*, which is involved in polarization of the cytoskeleton during the cell cycle (Holly and Blumer, 1999). Evidence for an involvement of actin in tip splitting was reported in studies of other filamentous fungi in which tip splitting was not observed in wild type but was seen in different mutants as a neomorphic phenotype. For example, the ramosa-1 mutant of *Aspergillus niger* can divide at hyphal tips when shifted to the restrictive temperature (Reynaga-Pena and Bartnicki-Garcia, 1997), and the authors suggested that tip splitting might be triggered by a transient alteration in the cytoskeletal organization. Similarly, viable mutations in the formin SepA in *A. nidulans* show tip splitting (Sharpless and Harris, 2002). In *Neurospora crassa*, several mutants are known that lead to hyphal tip splitting (Sone and Griffiths, 1999; Bok *et al.*, 2001; Seiler and Plamann, 2003; Virag and Griffiths, 2004). It was suggested that a calcium gradient controls the transport of vesicles. This control mechanism also involves actin and determines whether a tip divides or not. The increased surface expansion rate in *A. gossypii* hyphae with an activated allele of *AgBNI1*, reported here, is most likely caused by the increase in actin cables and thus vesicle transport. This overstimulation in vesicle transport also leads to premature tip splitting. The fact that GTP-bound *Ag*Cdc42p interacts with *Ag*Bni1p in a two-hybrid assay and that mutants expressing the activated allele of *AgCDC42* also show premature tip splitting suggest that this event is regulated by an *Ag*Bni1p branch of the *Ag*Cdc42p signaling network. The observed growth problems of the activated *Agcdc42* mutant compared with the activated *Agbni1* mutant can be explained by the fact that changes in the activity state of *Ag*Cdc42p will influence the interaction with multiple effector proteins (Nelson *et al.*, 2003).

The involvement of the Cdc42 GTPase in tip splitting is also supported by mutants described for the CDC24 homolog of *N. crassa* (Seiler and Plamann, 2003) because Cdc24p is a GDP-GTP exchange factor for the small GTPase Cdc42p.

On the basis of the data discussed here, we suggest a molecular model for tip splitting regulation. *Ag*Cdc42p activates *Ag*Bni1p which in turn increases the number of actin cables emanating from the tip. This leads than to a stimulation of actin cable-based vesicle transport, which first enlarges and finally divides the polar growth site into two new sites. These data, when combined, suggest that altering the activities of formin molecules by Cdc42p can lead to dramatically different cell shapes. Incorporation of future experiments into this model should help to increase our understanding of this unique process like e.g., its growth speed dependence or it might help us to understand in more detail how tip splitting is triggered.

Note added in proof. After submission of this manuscript, two other fungal formins, CaBni1p and CaBnr1p, were shown to play an important but nonessential role in yeast and hyphal growth of *Candida albicans* (Li *et al.*, 2005).

ACKNOWLEDGMENTS

We thank Sophie Brachat and Anne-Laure Vitte for their preliminary work on *Agbni1*Δ; Dominic Hoepfner and Anne L'Hernault for providing pUC19NatPS before publication; and Amy Gladfelter, Anja Lorberg, and Tom Bickle for critical reading of the manuscript. This work was supported by the University of Basel and the Swiss National Science Foundation Grant 3100A0-100734.

REFERENCES

Alberts, A. S. (2001). Identification of a carboxyl-terminal diaphanous-related formin homology protein autoregulatory domain. J. Biol. Chem. *276*, 2824–2830.

Altmann-Johl, R., and Philippsen, P. (1996). AgTHR4, a new selection marker for transformation of the filamentous fungus *Ashbya gossypii*, maps in a four-gene cluster that is conserved between *A. gossypii* and *Saccharomyces cerevisiae*. Mol. Gen. Genet. *250*, 69–80.

Ashby, S. F., and Nowell, W. (1926). The fungi of stigmatomycosis. Ann. Botany *40*, 69–86.

Ayad-Durieux, Y., Knechtle, P., Goff, S., Dietrich, F., and Philippsen, P. (2000). A PAK-like protein kinase is required for maturation of young hyphae and septation in the filamentous ascomycete *Ashbya gossypii*. J. Cell Sci. *113* (Pt 24), 4563–4575.

Bartel, P. L., Chien, C.-T., Sternglanz, R., and Fields, S. (1993). Using the two-hybrid system to detect protein-protein interactions. In: Cellular Interactions in Development: A Practical Approach, ed. D. A. Hartley, Oxford: Oxford University Press, 153–179.

Bauer, Y., Knechtle, P., Wendland, J., Helfer, H., and Philippsen, P. (2004). A Ras-like GTPase is involved in hyphal growth guidance in the filamentous fungus *Ashbya gossypii*. Mol. Biol. Cell *15*, 4622–4632.

Bobola, N., Jansen, R. P., Shin, T. H., and Nasmyth, K. (1996). Asymmetric accumulation of Ash1p in postanaphase nuclei depends on a myosin and restricts yeast mating-type switching to mother cells. Cell *84*, 699–709.

Bok, J. W., Sone, T., Silverman-Gavrila, L. B., Lew, R. R., Bowring, F. J., Catcheside, D. E., and Griffiths, A. J. (2001). Structure and function analysis of the calcium-related gene spray in *Neurospora crassa*. Fungal Genet. Biol. *32*, 145–158.

Boles, E., and Miosga, T. (1995). A rapid and highly efficient method for PCR-based site-directed mutagenesis using only one new primer. Curr. Genet. *28*, 197–198.

Caviston, J. P., Tcheperegine, S. E., and Bi, E. (2002). Singularity in budding: a role for the evolutionarily conserved small GTPase Cdc42p. Proc. Natl. Acad. Sci. USA *99*, 12185–12190.

Chang, F., Drubin, D., and Nurse, P. (1997). cdc12p, a protein required for cytokinesis in fission yeast, is a component of the cell division ring and interacts with profilin. J. Cell Biol. *137*, 169–182.

Dietrich, F. S. *et al.* (2004). The *Ashbya gossypii* genome as a tool for mapping the ancient *Saccharomyces cerevisiae* genome. Science *304*, 304–307.

Evangelista, M., Blundell, K., Longtine, M. S., Chow, C. J., Adames, N., Pringle, J. R., Peter, M., and Boone, C. (1997). Bni1p, a yeast formin linking cdc42p and the actin cytoskeleton during polarized morphogenesis. Science *276*, 118–122.

Evangelista, M., Pruyne, D., Amberg, D. C., Boone, C., and Bretscher, A. (2002). Formins direct Arp2/3-independent actin filament assembly to polarize cell growth in yeast. Nat. Cell Biol. *4*, 260–269.

Evangelista, M., Zigmond, S., and Boone, C. (2003). Formins: signaling effectors for assembly and polarization of actin filaments. J. Cell Sci. *116*, 2603–2611.

Feierbach, B., and Chang, F. (2001). Roles of the fission yeast formin for3p in cell polarity, actin cable formation and symmetric cell division. Curr. Biol. *11*, 1656–1665.

Gietz, R. D., and Sugino, A. (1988). New yeast-*Escherichia coli* shuttle vectors constructed with in vitro mutagenized yeast genes lacking six-base pair restriction sites. Gene *74*, 527–534.

Gow, N.A.R. (1995). Tip Growth and Polarity. In: The Growing Fungus, ed. N.A.R. Gow, G. M. Gadd, London: Chapman and Hall, 277–299.

Habas, R., Kato, Y., and He, X. (2001). Wnt/Frizzled activation of Rho regulates vertebrate gastrulation and requires a novel Formin homology protein Daam1. Cell *107*, 843–854.

Hanahan, D. (1983). Studies on transformation of *Escherichia coli* with plasmids. J. Mol. Biol. *166*, 557–580.

Harris, E. S., Li, F., and Higgs, H. N. (2004). The mouse formin, FRLalpha, slows actin filament barbed end elongation, competes with capping protein, accelerates polymerization from monomers, and severs filaments. J. Biol. Chem. *279*, 20076–20087.

Harris, S. D., Read, N. D., Roberson, R. W., Shaw, B., Seiler, S., Plamann, M., and Momany, M. (2005). Polarisome meets spitzenkorper: microscopy, genetics, and genomics converge. Eukaryot. Cell *4*, 225–229.

Harris, S. D., Hamer, L., Sharpless, K. E., and Hamer, J. E. (1997). The *Aspergillus nidulans* sepA gene encodes an FH1/2 protein involved in cytokinesis and the maintenance of cellular polarity. EMBO J. *16*, 3474–3483.

Higgs, H. N., and Peterson, K. J. (2005). Phylogenetic analysis of the formin homology 2 domain. Mol. Biol. Cell *16*, 1–13.

Hill, K. L., Catlett, N. L., and Weisman, L. S. (1996). Actin and myosin function in directed vacuole movement during cell division in *Saccharomyces cerevisiae*. J. Cell Biol. *135*, 1535–1549.

Hoepfner, D., van den Berg, M., Philippsen, P., Tabak, H. F., and Hettema, E. H. (2001). A role for Vps1p, actin, and the Myo2p motor in peroxisome abundance and inheritance in *Saccharomyces cerevisiae*. J. Cell Biol. *155*, 979–990.

Holly, S. P., and Blumer, K. J. (1999). PAK-family kinases regulate cell and actin polarization throughout the cell cycle of *Saccharomyces cerevisiae*. J. Cell Biol. *147*, 845–856.

Imamura, H., Tanaka, K., Hihara, T., Umikawa, M., Kamei, T., Takahashi, K., Sasaki, T., and Takai, Y. (1997). Bni1p and Bnr1p: downstream targets of the Rho family small G-proteins which interact with profilin and regulate actin cytoskeleton in *Saccharomyces cerevisiae*. EMBO J. *16*, 2745–2755.

James, P., Halladay, J., and Craig, E. A. (1996). Genomic libraries and a host strain designed for highly efficient two-hybrid selection in yeast. Genetics *144*, 1425–1436.

Johnston, G. C., Prendergast, J. A., and Singer, R. A. (1991). The *Saccharomyces cerevisiae MYO2* gene encodes an essential myosin for vectorial transport of vesicles. J. Cell Biol. *113*, 539–551.

Kamei, T., Tanaka, K., Hihara, T., Umikawa, M., Imamura, H., Kikyo, M., Ozaki, K., and Takai, Y. (1998). Interaction of Bnr1p with a novel Src homology 3 domain-containing Hof1p. Implication in cytokinesis in *Saccharomyces cerevisiae*. J. Biol. Chem. *273*, 28341–28345.

Knechtle, P., Dietrich, F., and Philippsen, P. (2003). Maximal polar growth potential depends on the polarisome component AgSpa2 in the filamentous fungus *Ashbya gossypii*. Mol. Biol. Cell *14*, 4140–4154.

Kobielak, A., Pasolli, H. A., and Fuchs, E. (2003). Mammalian formin-1 participates in adherens junctions and polymerization of linear actin cables. Nat. Cell Biol. *6*, 21–30.

Kohno, H. *et al.* (1996). Bni1p implicated in cytoskeletal control is a putative target of Rho1p small GTP binding protein in *Saccharomyces cerevisiae*. EMBO J. *15*, 6060–6068.

Kovar, D. R., Kuhn, J. R., Tichy, A. L., and Pollard, T. D. (2003). The fission yeast cytokinesis formin Cdc12p is a barbed end actin filament capping protein gated by profilin. J. Cell Biol. *161*, 875–887.

Li, C. R., Wang, Y. M., DeZheng, X., Liang, H. Y., Tang, J. C., and Wang, Y. (2005). The formin family protein CaBni1p has a role in cell polarity control during both yeast and hyphal growth in *Candida albicans*. J. Cell. Sci. *118*, 2637–2648.

Li, F., and Higgs, H. N. (2003). The mouse Formin mDia1 is a potent actin nucleation factor regulated by autoinhibition. Curr. Biol. *13*, 1335–1340.

Momany, M. (2002). Polarity in filamentous fungi: establishment, maintenance and new axes. Curr. Opin. Microbiol. *5*, 580–585.

Moseley, J. B., Sagot, I., Manning, A. L., Xu, Y., Eck, M. J., Pellman, D., and Goode, B. L. (2004). A conserved mechanism for Bni1- and mDia1-induced actin assembly and dual regulation of Bni1 by Bud6 and profilin. Mol. Biol. Cell *15*, 896–907.

Nakano, K., Imai, J., Arai, R., Toh, E. A., Matsui, Y., and Mabuchi, I. (2002). The small GTPase Rho3 and the diaphanous/formin For3 function in polarized cell growth in fission yeast. J. Cell Sci. *115*, 4629–4639.

Needleman, S. B., and Wunsch, C. D. (1970). A general method applicable to the search for similarities in the amino acid sequence of two proteins. J. Mol. Biol. *48*, 443–453.

Nelson, B. *et al.* (2003).. RAM: a conserved signaling network that regulates Ace2p transcriptional activity and polarized morphogenesis. Mol. Biol. Cell *14*, 3782–3803.

Ozaki-Kuroda, K., Yamamoto, Y., Nohara, H., Kinoshita, M., Fujiwara, T., Irie, K., and Takai, Y. (2001). Dynamic localization and function of Bni1p at the sites of directed growth in *Saccharomyces cerevisiae*. Mol. Cell. Biol. *21*, 827–839.

Pearson, W. R. (1990). Rapid and sensitive sequence comparison with FASTP and FASTA. Methods Enzymol. *183*, 63–98.

Petersen, J., Nielsen, O., Egel, R., and Hagan, I. M. (1998a). F-actin distribution and function during sexual differentiation in *Schizosaccharomyces pombe*. J. Cell Sci. *111 (Pt 7)*, 867–876.

Petersen, J., Nielsen, O., Egel, R., and Hagan, I. M. (1998b). FH3, a domain found in formins, targets the fission yeast formin Fus1 to the projection tip during conjugation. J. Cell Biol. *141*, 1217–1228.

Pruyne, D., Evangelista, M., Yang, C., Bi, E., Zigmond, S., Bretscher, A., and Boone, C. (2002). Role of formins in actin assembly: nucleation and barbed-end association. Science *297*, 612–615.

Pruyne, D., Gao, L., Bi, E., and Bretscher, A. (2004). Stable and dynamic axes of polarity use distinct formin isoforms in budding yeast. Mol. Biol. Cell *15*, 4971–4989.

Reynaga-Pena, C. G., and Bartnicki-Garcia, S. (1997). Apical branching in a temperature sensitive mutant of *Aspergillus niger*. Fungal Genet. Biol. *22*, 153–167.

Rossanese, O. W., Reinke, C. A., Bevis, B. J., Hammond, A. T., Sears, I. B., O'Connor, J., and Glick, B. S. (2001). A role for actin, Cdc1p, and Myo2p in the inheritance of late Golgi elements in *Saccharomyces cerevisiae*. J. Cell Biol. *153*, 47–62.

Sagot, I., Klee, S. K., and Pellman, D. (2002a). Yeast formins regulate cell polarity by controlling the assembly of actin cables. Nat. Cell Biol. *4*, 42–50.

Sagot, I., Rodal, A. A., Moseley, J., Goode, B. L., and Pellman, D. (2002b). An actin nucleation mechanism mediated by Bni1 and profilin. Nat. Cell Biol. *4*, 626–631.

Sambrook, J., Russel, D. W., and Sambrook, J. (2001). Molecular Cloning: A Laboratory Manual, Cold Spring Harbor, NY: Cold Spring Harbor Laboratory.

Schott, D. H., Collins, R. N., and Bretscher, A. (2002). Secretory vesicle transport velocity in living cells depends on the myosin-V lever arm length. J. Cell Biol. *156*, 35–39.

Seiler, S., and Plamann, M. (2003). The genetic basis of cellular morphogenesis in the filamentous fungus *Neurospora crassa*. Mol. Biol. Cell *14*, 4352–4364.

Sharpless, K. E., and Harris, S. D. (2002). Functional characterization and localization of the *Aspergillus nidulans* formin SEPA. Mol. Biol. Cell *13*, 469–479.

Sheu, Y. J., Santos, B., Fortin, N., Costigan, C., and Snyder, M. (1998). Spa2p interacts with cell polarity proteins and signaling components involved in yeast cell morphogenesis. Mol. Cell. Biol. *18*, 4053–4069.

Shimada, A., Nyitrai, M., Vetter, I. R., Kuhlmann, D., Bugyi, B., Narumiya, S., Geeves, M. A., and Wittinghofer, A. (2004). The core FH2 domain of diaphanous-related formins is an elongated actin binding protein that inhibits polymerization. Mol. Cell *13*, 511–522.

Sikorski, R. S., and Hieter, P. (1989). A system of shuttle vectors and yeast host strains designed for efficient manipulation of DNA in *Saccharomyces cerevisiae*. Genetics *122*, 19–27.

Sil, A., and Herskowitz, I. (1996). Identification of asymmetrically localized determinant, Ash1p, required for lineage-specific transcription of the yeast *HO* gene. Cell *84*, 711–722.

Simon, V. R., Swayne, T. C., and Pon, L. A. (1995). Actin-dependent mitochondrial motility in mitotic yeast and cell-free systems: identification of a motor activity on the mitochondrial surface. J. Cell Biol. *130*, 345–354.

Sone, T., and Griffiths, A. J. (1999). The frost gene of *Neurospora crassa* is a homolog of yeast *cdc1* and affects hyphal branching via manganese homeostasis. Fungal Genet. Biol. *28*, 227–237.

Steiner, S., and Philippsen, P. (1994). Sequence and promoter analysis of the highly expressed *TEF* gene of the filamentous fungus *Ashbya gossypii*. Mol. Gen. Genet. *242*, 263–271.

Steiner, S., Wendland, J., Wright, M. C., and Philippsen, P. (1995). Homologous recombination as the main mechanism for DNA integration and cause of rearrangements in the filamentous ascomycete *Ashbya gossypii*. Genetics *140*, 973–987.

Storici, F., Lewis, L. K., and Resnick, M. A. (2001). In vivo site-directed mutagenesis using oligonucleotides. Nat. Biotechnol. *19*, 773–776.

Takizawa, P. A., DeRisi, J. L., Wilhelm, J. E., and Vale, R. D. (2000). Plasma membrane compartmentalization in yeast by messenger RNA transport and a septin diffusion barrier. Science *290*, 341–344.

Vieira, J., and Messing, J. (1991). New pUC-derived cloning vectors with different selectable markers and DNA replication origins. Gene *100*, 189–194.

Virag, A., and Griffiths, A. J. (2004). A mutation in the *Neurospora crassa* actin gene results in multiple defects in tip growth and branching. Fungal Genet. Biol. *41*, 213–225.

Wallar, B. J., and Alberts, A. S. (2003). The formins: active scaffolds that remodel the cytoskeleton. Trends Cell Biol. *13*, 435–446.

Watanabe, N., Kato, T., Fujita, A., Ishizaki, T., and Narumiya, S. (1999). Cooperation between mDia1 and ROCK in Rho-induced actin reorganization. Nat. Cell Biol. *1*, 136–143.

Watanabe, N., Madaule, P., Reid, T., Ishizaki, T., Watanabe, G., Kakizuka, A., Saito, Y., Nakao, K., Jockusch, B. M., and Narumiya, S. (1997). p140mDia, a mammalian homolog of *Drosophila* diaphanous, is a target protein for Rho small GTPase and is a ligand for profilin. EMBO J. *16*, 3044–3056.

Wendland, J., Ayad-Durieux, Y., Knechtle, P., Rebischung, C., and Philippsen, P. (2000). PCR-based gene targeting in the filamentous fungus *Ashbya gossypii*. Gene *242*, 381–391.

Wendland, J., and Philippsen, P. (2000). Determination of cell polarity in germinated spores and hyphal tips of the filamentous ascomycete *Ashbya gossypii* requires a rhoGAP homolog. J. Cell Sci. *113*(Pt 9), 1611–1621.

Wendland, J., and Philippsen, P. (2001). Cell polarity and hyphal morphogenesis are controlled by multiple rho-protein modules in the filamentous ascomycete *Ashbya gossypii*. Genetics *157*, 601–610.

Wright, M. C., and Philippsen, P. (1991). Replicative transformation of the filamentous fungus *Ashbya gossypii* with plasmids containing *Saccharomyces cerevisiae* ARS elements. Gene *109*, 99–105.

Xu, Y., Moseley, J. B., Sagot, I., Poy, F., Pellman, D., Goode, B. L., and Eck, M. J. (2004). Crystal structures of a Formin Homology-2 domain reveal a tethered dimer architecture. Cell *116*, 711–723.

Zahner, J. E., Harkins, H. A., and Pringle, J. R. (1996). Genetic analysis of the bipolar pattern of bud site selection in the yeast *Saccharomyces cerevisiae*. Mol. Cell. Biol. *16*, 1857–1870.